

# Palladium-Mediated CO<sub>2</sub> Extrusion Followed by Insertion of Isocyanates for the Synthesis of Benzamides: Translating Fundamental Mechanistic Studies To Develop a Catalytic Protocol

Yang Yang, Allan J. Canty, Alasdair I. McKay, Paul S. Donnelly, and Richard A. J. O'Hair\*



Cite This: <https://dx.doi.org/10.1021/acs.organomet.9b00820>



Read Online

ACCESS |



Metrics & More

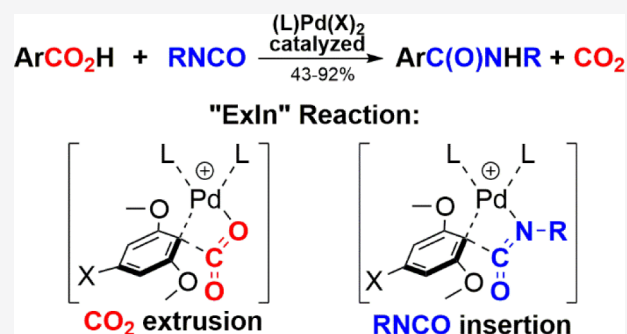


Article Recommendations



Supporting Information

**ABSTRACT:** Mechanistic studies of a stoichiometric palladium-mediated ExIn (ExIn = extrusion–insertion) decarboxylative amidation of aromatic carboxylic acids are presented, providing gas-phase and condensed-phase spectroscopic data, as well as theoretical computational evidence for intermediates in a proposed stepwise process. The understanding gained from these mechanistic studies directed the development of a palladium-catalyzed procedure in which benzamides are obtained in good to high yields in a one-pot 30 min microwave irradiation assisted protocol. A combination of experimental data and DFT calculations reveals that certain ligand additives favor the selective formation of benzamides rather than the undesired protodecarboxylation side product.

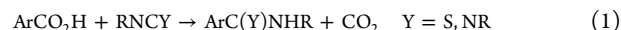


## INTRODUCTION

The amide functional group is arguably the most important structural motif in biology and chemistry. Nature uses amide bonds within natural products, peptides, and proteins. Amide bonds are also found in one out of four of all pharmaceuticals on the market, as well as synthetic agrochemicals and functional materials.<sup>1</sup> The preparation of amides by the condensation of carboxylic acids and primary amines is one of the most widely used chemical reactions in contemporary synthetic chemistry.<sup>2</sup> However, forcing conditions are typically employed, which limits the applicability to very robust substrates. Stoichiometric coupling reagents, such as HATU (1-[bis(dimethylamino)-methylene]-1H-1,2,3-triazolo[4,5-*b*]pyridinium-3-oxide hexafluorophosphate, Scheme 1A), have been developed to overcome these limitations.<sup>3</sup> While they are widely used, such protocols produce stoichiometric amounts of waste, which complicates the isolation of the desired amide product.<sup>4,5</sup> New methods for amide formation that overcome this poor atom economy by activating alternative bonds are highly desirable and form the basis of several new strategies that include C–B and C–H bond activation.<sup>6–8</sup>

We previously coined the term “ExIn” (extrusion–insertion) to describe a new class of reactions for thioamide and amidine synthesis (eq 1, Y = S, NR). In these isohypsic protocols palladium(II) complexes mediate the decarboxylation of an aromatic carboxylic acid, affording an organopalladium(II) intermediate which subsequently inserts either an isothiocyanate or a carbodiimide followed by demetalation to afford the thioamide (Scheme 1B, Y = S)<sup>9</sup> or amidine (Scheme 1B, Y =

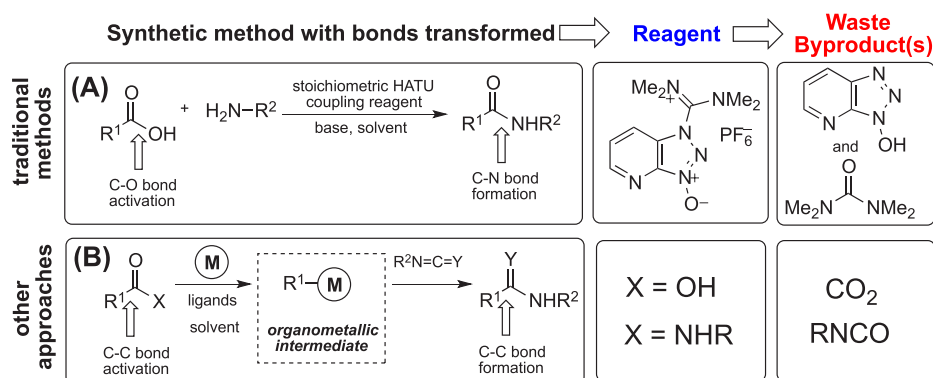
NR).<sup>10</sup> The decarboxylation and insertion steps are directly related, as CO<sub>2</sub>, RNCS, and RNCNR are all isoelectronic.



In this report, we extend the scope of the ExIn class of reactions to target the synthesis of benzamides (Scheme 1B, Y = O) with the aim of developing an atom-efficient catalytic procedure (Scheme 2). We restricted our study to 2,6-dimethoxy- and 2,4,6-trimethoxybenzoic acids, as monosubstituted benzoic acids can undergo undesirable side reactions involving Pd-mediated C–H bond activation at the positions ortho to the carboxylate group.<sup>12,13</sup> Although not a key motivation for our work, it is worth noting that the trimethoxybenzamide functional group has been demonstrated recently to produce molecules that are selective inhibitors of P-glycoprotein.<sup>14</sup> Available thermochemical data suggest that the formation of an amide via an ExIn reaction (eq 1, Y = O) is exothermic by over 20 kcal/mol,<sup>15</sup> with release of gaseous CO<sub>2</sub> providing a further driving force. The key steps are likely to involve binding of the carboxylate to the metal ion (eq 2, Scheme 2), decarboxylation (eq 3, Scheme 2),<sup>16,17</sup> insertion of the isocyanate, RNCO, into the Pd–C bond (eq 4, Scheme 2) affording the amidate complex 4,<sup>18–20</sup> and release of the amide 5 from the metal ion (eq 5, Scheme 2). While many of these

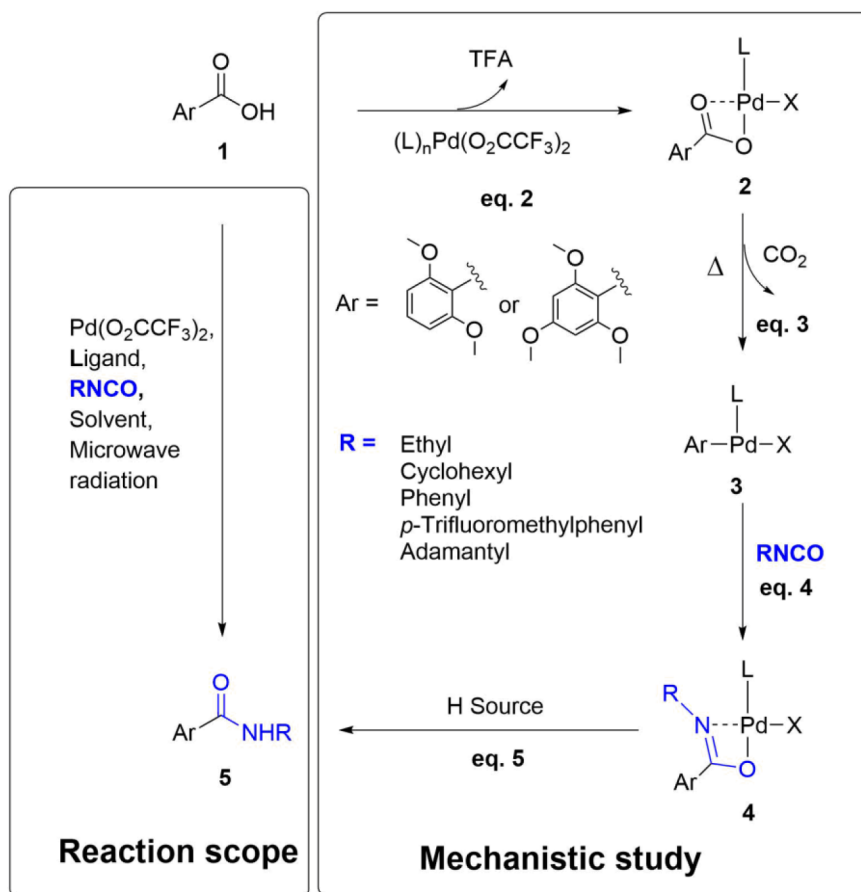
Received: December 2, 2019

Scheme 1. Methods for Amide Synthesis: (A) C–OH Bond Activation Followed by C–N Bond Formation; (B) ExIn Approach Involving C–C Bond Activation To Form an Organometallic Intermediate Followed by Insertion<sup>a</sup>



<sup>a</sup>X = OH, Y = S, see ref 9; X = OH, Y = NR, see ref 10; X = NHR, Y = O, see ref 11; X = OH, Y = O, this work.

Scheme 2. Reaction Scope of Catalytic Reactions (Left Column) and Mechanistic Study for the Synthesis of Amides Modeled on the ExIn Protocol (Right Column)

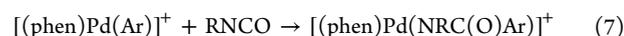
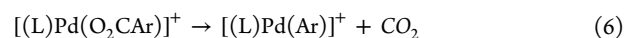


individual steps have precedents, they have not been used together to achieve a catalytic synthesis of benzamides directly from benzoic acids (eq 1, Y = O).

## RESULTS AND DISCUSSION

**Gas-Phase Studies of the Decarboxylation and Isocyanate Insertion Steps.** Multistage mass spectrometry ( $MS^n$ ) experiments in a linear ion trap mass spectrometer and DFT calculations were used to examine the key steps associated with the transformation of palladium-ligated

benzoate to palladium-ligated amidate in the gas phase (eqs 6 and 7).



We have previously shown that the organometallic cation  $[(phen)Pd(Ar)]^+$  (9a, Figure 1a, phen = 1,10-phenanthroline) can be generated by collision-induced dissociation (CID) of  $CO_2$  from  $[(phen)Pd(O_2CAr)]^+$  (6a).<sup>9</sup> Decarboxylation is also readily observed when the phen ligand is replaced by the more

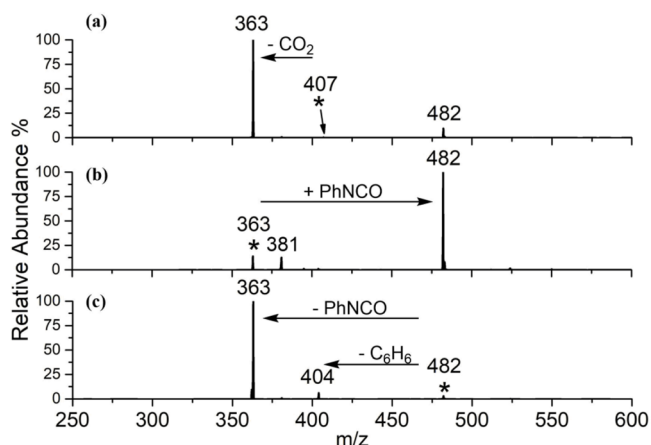
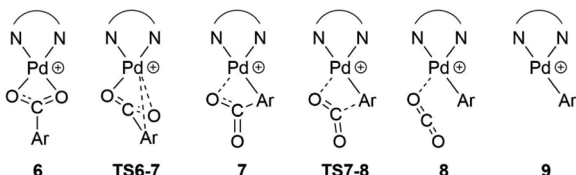


**Figure 1.** LTQ MS<sup>n</sup> spectra of unimolecular and bimolecular reactions associated with key steps of the ExIn reaction: (a) MS<sup>2</sup> experiment involving extrusion of CO<sub>2</sub> from [(phen)Pd(O<sub>2</sub>CC<sub>6</sub>H<sub>5</sub>)]<sup>+</sup> (*m/z* 407) under CID at a normalized collision energy of 20 (eq 6); (b) MS<sup>3</sup> experiment involving an ion–molecule reaction between the organometallic ion [(phen)Pd(C<sub>6</sub>H<sub>5</sub>)]<sup>+</sup> (*m/z* 363) and phenyl isocyanate (reaction time 300 ms) (eq 7); (c) MS<sup>4</sup> experiment involving CID on selected IMR product (*m/z* 482) at a normalized collision energy of 20 (eq 7). The concentration of PhNCO in the ion–molecule reaction is  $1.1 \times 10^{10}$  molecules cm<sup>-3</sup>. The mass-selected ions are denoted by asterisks.

flexible 2,2-bipyridine (bpy) or 6-methyl-2,2-bipyridine (6mbpy) to afford the organometallic cations **9c,e**, respectively (Figure S1). In these instances, “rollover” cyclometalated complexes were also formed as minor products (Figure S1).

The effect of the identity of the ligand and benzoic acid on decarboxylation were investigated using density functional theory (DFT) computation. These studies show that all combinations of ligand and benzoic acid proceed via the same pathway (Scheme 3 and Figure S2) in an endergonic manner.

### Scheme 3. General Mechanism for Extrusion of CO<sub>2</sub> as in Eq 6<sup>a</sup>



<sup>a</sup>Specific systems studied: (a) N–N = phen and Ar = C<sub>6</sub>H<sub>5</sub> (ref 9); (b) N–N = phen and Ar = 2,6-(CH<sub>3</sub>O)<sub>2</sub>C<sub>6</sub>H<sub>3</sub> (ref 10); (c) N–N = bpy and Ar = C<sub>6</sub>H<sub>5</sub> (this work); (d) N–N = bpy and Ar = 2,6-(CH<sub>3</sub>O)<sub>2</sub>C<sub>6</sub>H<sub>3</sub> (this work); (e) N–N = 6mbpy and Ar = C<sub>6</sub>H<sub>5</sub> (this work); (f) N–N = 6mbpy and Ar = 2,6-(CH<sub>3</sub>O)<sub>2</sub>C<sub>6</sub>H<sub>3</sub> (this work).

The identity of the ligand was found to have a negligible effect on the energetics (Table 1). In contrast, replacing benzoic acid with 2,6-dimethoxybenzoic acid resulted in intermediates and TS7-8 lying at significantly lower energies and the overall reaction became less endergonic (Scheme 3, Figure S3, and Table 1). There are many literature reports of ortho-substituted benzoic acid derivatives undergoing more facile decarboxylation relative to their unsubstituted counterparts.<sup>23</sup> The rollover cyclometalation pathway from **6c** was also calculated (Figure S2), and it is considerably less kinetically and thermodynamically accessible, consistent with it being a minor experimental product.

The gas-phase ion–molecule reactions (IMR) between the coordinatively unsaturated organometallic ions **9** and phenyl isocyanate were investigated (eq 7). Inspection of key spectra (Figure 1b and Figure S4), and kinetic data (Table 2) reveals

**Table 2. Absolute Rates and Reaction Efficiencies of Ion–Molecule Reactions between [(L)Pd(Ar)]<sup>+</sup> and Phenyl Isocyanate (Eq 7)**

reactant ion	absolute rate/ $10^{-10}$ cm <sup>3</sup> molecules <sup>-1</sup> s <sup>-1</sup>	reaction efficiency/%
(a) [(phen)Pd(C <sub>6</sub> H <sub>5</sub> )] <sup>+</sup>	0.88	8
(b) [(phen)Pd((CH <sub>3</sub> O) <sub>2</sub> C <sub>6</sub> H <sub>3</sub> )] <sup>+</sup>	no reaction	
(c) [(bpy)Pd(C <sub>6</sub> H <sub>5</sub> )] <sup>+</sup>	9.6	79
(d) [(bpy)Pd((CH <sub>3</sub> O) <sub>2</sub> C <sub>6</sub> H <sub>3</sub> )] <sup>+</sup>	no reaction	
(e) [(6mbpy)Pd(C <sub>6</sub> H <sub>5</sub> )] <sup>+</sup>	2.4	20
(f) [(6mbpy)Pd((CH <sub>3</sub> O) <sub>2</sub> C <sub>6</sub> H <sub>3</sub> )] <sup>+</sup>	no reaction	

that [(phen)Pd(C<sub>6</sub>H<sub>5</sub>)]<sup>+</sup> (**9a**) reacts at a rate of  $8.8 \times 10^{-11}$  cm<sup>3</sup> molecules<sup>-1</sup> s<sup>-1</sup>, corresponding to a reaction efficiency of 8% to afford an ion at *m/z* 482 as the major product ion (Figure 1b and eq 7, Ar = C<sub>6</sub>H<sub>5</sub>). This product ion corresponds to either the amidate complex [(phen)Pd(NPhC(O)Ph)]<sup>+</sup> or the isocyanate adduct [(phen)Pd(PhNCO)(Ph)]<sup>+</sup>. The CID spectrum of this product ion is very similar to that of palladium benzamidate, prepared by mixing *N*-phenylbenzamide, palladium trifluoroacetate, and phen in methanol (Figure S5b).<sup>24</sup> Both CID processes proceed via two different fragmentation channels: (a) loss of phenyl isocyanate to re-form the organometallic ion **6** as the major pathway (Figure 1c and eq 8) and (b) loss of benzene to produce an ion at *m/z* 404 as a minor pathway (Figure 1c and eq 9). Deuterium labeling studies in which CID of the product formed by the IMR of [(phen)Pd(C<sub>6</sub>D<sub>5</sub>)]<sup>+</sup> and phenyl isocyanate proceeded via loss of C<sub>6</sub>D<sub>5</sub>H (Figure S6) confirm that arene loss originates from the benzoic acid and not the phenyl isocyanate.

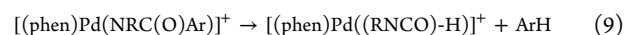
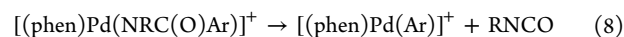


**Table 1. DFT Data of Relative Gibbs Energies and Enthalpies (In Parentheses) Given in kcal/mol for the Species Associated with Extrusion of CO<sub>2</sub> Shown in Scheme 3 (Eq 6)**

system	6	TS6-7	7	TS7-8	8	9
(a) [(phen)Pd(C <sub>6</sub> H <sub>5</sub> )] <sup>+</sup> <sup>a</sup>	0.0 (0.0)	34.9 (35.1)	15.3 (15.2)	27.1 (27.9)	9.3 (12.0)	<i>b</i>
(b) [(phen)Pd((CH <sub>3</sub> O) <sub>2</sub> C <sub>6</sub> H <sub>3</sub> )] <sup>+</sup> <sup>c</sup>	0.0 (0.0)	35.9 (34.4)	4.0 (4.0)	12.0 (10.1)	0.1 (1.8)	4.9 (16.6)
(c) [(bpy)Pd(C <sub>6</sub> H <sub>5</sub> )] <sup>+</sup>	0.0 (0.0)	36.2 (35.2)	17.8 (16.0)	26.9 (27.1)	9.5 (12.4)	13.4 (25.9)
(d) [(bpy)Pd((CH <sub>3</sub> O) <sub>2</sub> C <sub>6</sub> H <sub>3</sub> )] <sup>+</sup>	0.0 (0.0)	37.1 (35.2)	5.4 (4.7)	11.3 (11.6)	2.7 (3.6)	6.8 (18.6)

<sup>a</sup>From ref 9. <sup>b</sup>Not calculated. <sup>c</sup>From ref 10.

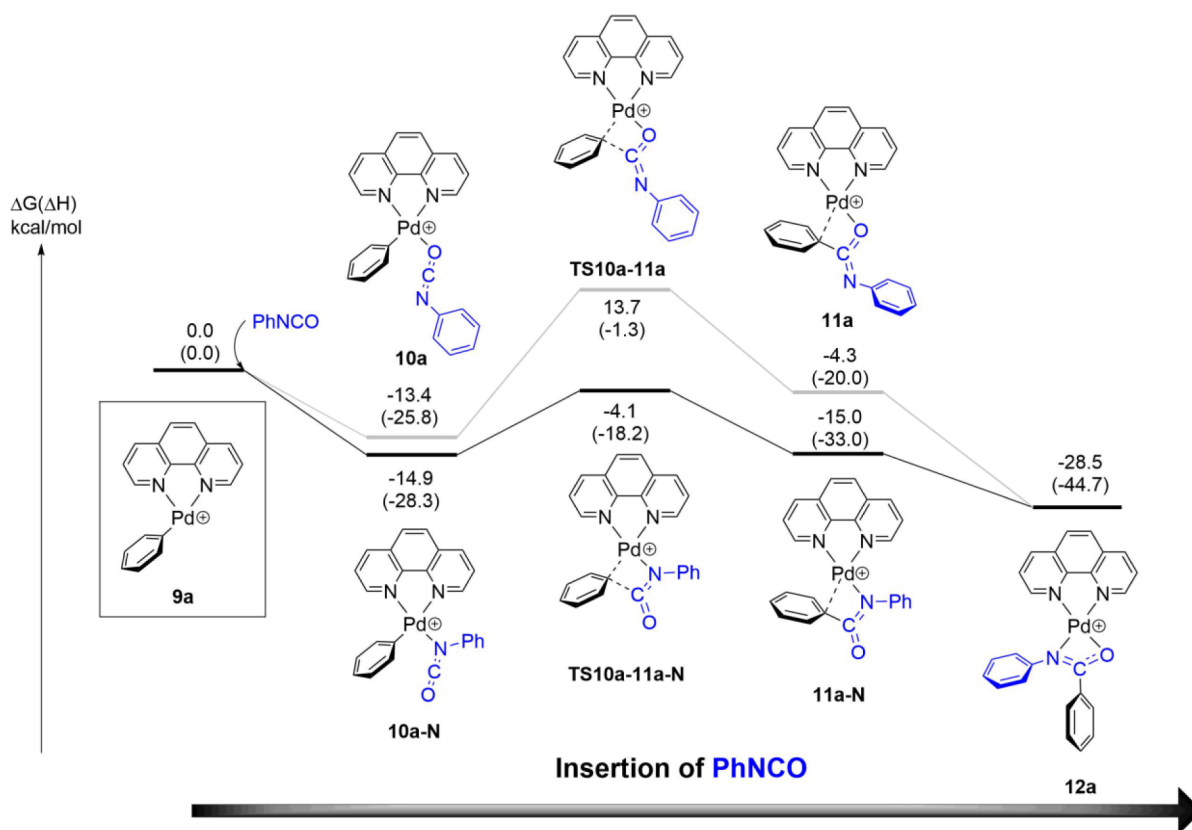


**Figure 2.** DFT calculated energy surface for reaction of  $[(\text{phen})\text{Pd}(\text{C}_6\text{H}_5)]^+$  (**9a**) with phenyl isocyanate (eq 7). The relative Gibbs energies and enthalpies (in parentheses) are given in kcal/mol and were calculated at the B3LYP-D3BJ/BS2//M06/BS1 level of theory.

**Table 3.** DFT Data of Relative Gibbs Energies and Enthalpies (in Parentheses) Given in kcal/mol for the Species in the Insertion Reactions of  $[(\text{L})\text{Pd}(\text{C}_6\text{H}_5)]^+$  and Phenyl Isocyanate

system	coordination mode	9	10	TS10-11	11	12
(a) $[(\text{phen})\text{Pd}(\text{C}_6\text{H}_5)]^+$	Pd–O	0.0 (0.0)	–13.4 (–25.8)	13.7 (–1.3)	–4.3 (–20.0)	–28.5 (–44.7)
	Pd–N	0.0 (0.0)	–14.9 (–28.3)	–4.1 (–18.2)	–15.0 (–33.0)	–28.5 (–44.7)
(c) $[(\text{bpy})\text{Pd}(\text{C}_6\text{H}_5)]^+$	Pd–O	0.0 (0.0)	–12.7 (–26.0)	12.1 (–2.3)	–5.9 (–21.3)	–30.9 (–46.5)
	Pd–N	0.0 (0.0)	–17.3 (–29.6)	–3.3 (–18.6)	–16.3 (–31.6)	–30.9 (–46.5)

Both **9c** and **9e** react more readily with phenyl isocyanate ( $9.6 \times 10^{-10}$  and  $2.4 \times 10^{-10}$   $\text{cm}^3 \text{molecules}^{-1} \text{s}^{-1}$ , respectively). These reactions are notably more efficient (79% and 20%, respectively) than the reaction starting from **9a** (8%), indicating a lower barrier for phenyl isocyanate insertion in the bpy-ligated complexes relative to the phen-ligated complex. There is no reaction with phenyl isocyanate when we replaced benzoic acid (systems a, c, and e) with 2,6-dimethoxybenzoic acid (systems b, d, and f) (Table 2).

DFT calculations on the insertion step (Figure 2) predict the reaction of  $[(\text{phen})\text{Pd}(\text{C}_6\text{H}_5)]^+$  (**9a**) and phenyl isocyanate to initially afford the N-coordinated phenyl isocyanate adduct (**10a-N**). Binding of the phenyl isocyanate via the oxygen (**10a**) is both kinetically and thermodynamically less favorable (Table 3). Subsequent C–C bond formation via transition structure **TS10c-11c-N** affords the  $\kappa^2$ -N,C-benzamide complex (**11a-N**). The energy of transition structure **TS10c-11c-N** lies below that of the starting reagents, indicating that C–C bond formation is kinetically accessible under ion–molecule reaction conditions, supporting our earlier assignment of the product ion as an amidate complex rather than an isocyanate adduct. Structure **11a-N** sub-

sequently isomerizes to the more stable  $\kappa^2$ -N,O-benzamide structure (**12a**). This mode of amidate binding to palladium has precedence in other structurally characterized group 10 complexes.<sup>25,26</sup> The overall reaction of **9a** with phenyl isocyanate to afford **12a** is predicted to be highly exothermic and exergonic. With bpy ligation, an analogous mechanism is computed (Figure S7). However, lower barriers are calculated relative to the phen-ligated system, consistent with the experimentally determined relative reaction efficiencies (Table 3). DFT calculations also predict lower kinetic barriers for the phenyl isocyanate insertion into the methoxy-substituted intermediates **9b,d** (Figures S8 and S9). However, in both cases lower energy isomers of **9b** and **9d** are located, where one of the *o*-methoxy substituents binds to the vacant site on palladium, cf. **9b2,d2** (Figures S8 and S9), thereby blocking coordination of phenyl isocyanate. These results are consistent with the poor reactivity observed experimentally for these systems (Table 2).

**Competition between Isocyanate and Arene Loss in the CID Reactions of Amidate Complexes  $[(\text{phen})\text{Pd}(\text{NRC}(\text{O})\text{Ar})]^+$ .** Given that the CID spectra of the authentic amidate complexes show two competing fragmentation

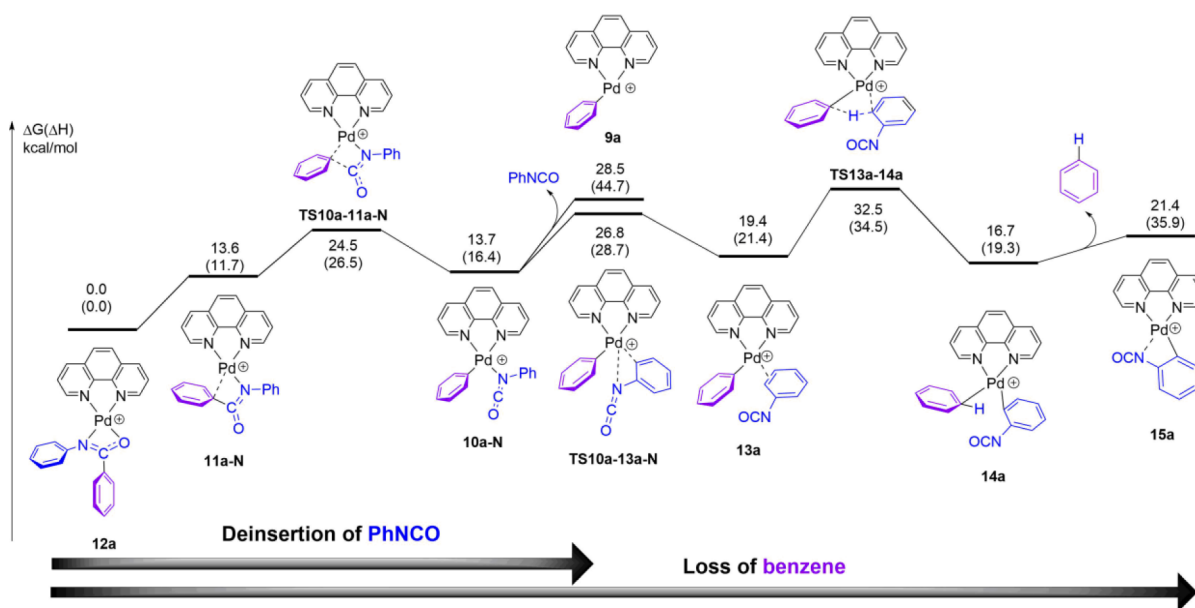
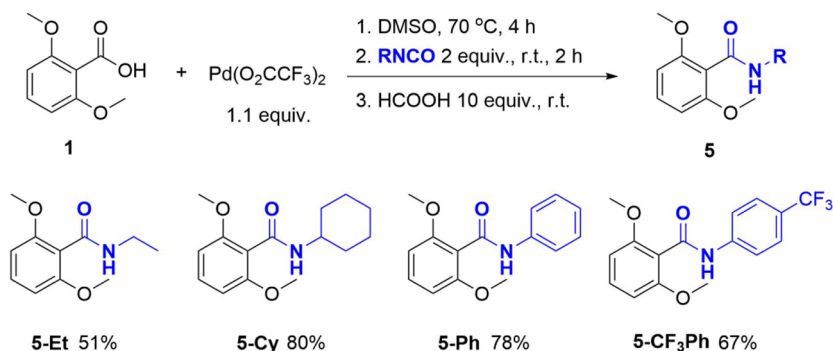


**Figure 3.** DFT calculated energy surface for fragmentation of  $[(\text{phen})\text{Pd}(\text{NPhC}(\text{O})\text{Ph})]^+$  (**12a**): deinsertion of PhNCO (eq 8) and loss of benzene from C–H bond activation (eq 7). The relative Gibbs and enthalpy energies (in parentheses) are given in kcal/mol and were calculated at the B3LYP-D3BJ/BS2//M06/BS1 level of theory.

#### Scheme 4. Scope of Stoichiometric Palladium-Mediated Decarboxylative Synthesis of Benzamides in Terms of the Isocyanate Substrates Used

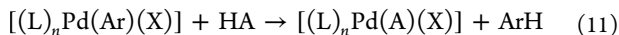
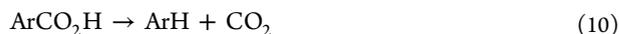


channels (eqs 8 and 9), we decided to probe their mechanisms via DFT calculations. The calculated fragmentation pathways starting from the  $\kappa^2$ -*N,O*-benzamidate structure, **12a**, are shown in Figure 3. Under the experimental low-energy CID conditions, the fragmentation reactions are under kinetic control and entropic effects play a role. While the exact temperature of the fragmenting ions is unknown, we use the DFT calculated Gibbs free energies at 298 K as the key thermochemical parameter when considering competing fragmentation pathways. Thus, while the loss of benzene rather than isocyanate is predicted to be thermodynamically favored by 8 kcal/mol, the benzene elimination pathway proceeds through a high barrier, **TS13a-14a**, making loss of phenyl isocyanate the kinetically favored pathway, consistent with the experimental outcome (Figure 1c).

**Condensed-Phase Studies To Isolate Amides and Explore Substrate Scope Using Stoichiometric Pd Salts under Ligand-Free Conditions.** Encouraged by the proof of concept gas-phase studies, we explored the conversion of 2,6-disubstituted benzoic acids into benzamides using a stoichiometric amount of palladium trifluoroacetate. Employing the conditions previously optimized for synthesis of amidines, 2,6-

dimethoxybenzoic acid was decarboxylated by palladium trifluoroacetate in DMSO at 70 °C for 4 h (Scheme 4). Subsequent addition of excess phenyl isocyanate at room temperature and protodemetalation with formic acid afforded *N*-phenyl-2,6-dimethoxybenzamide (**5-Ph**), as identified by HRMS of the crude reaction mixture. This compound was separated from the side products, 1,3-diphenylurea<sup>27</sup> and 1,3-dimethoxybenzene,<sup>28</sup> by column chromatography and isolated in good yield (Scheme 4). With the optimized reaction conditions in hand, we explored the scope of possible substrates with an electron-withdrawing aryl isocyanate, 4-(trifluoromethyl)phenyl isocyanate. The resultant amide, **5-CF<sub>3</sub>Ph**, was obtained in good yield (Scheme 4). Aliphatic isocyanates were also investigated and led to isolation of benzamide product in moderate to good yield (Scheme 4), with the exception of 1-adamantyl isocyanate. Interrogation of the crude reaction mixture revealed significant quantities of the protodecarboxylation side product (eq 10), formed via protonation of the organopalladium species (eq 11, where L = DMSO, X = CF<sub>3</sub>CO<sub>2</sub>, and HA = CF<sub>3</sub>CO<sub>2</sub>H),<sup>28</sup> accompanied by 1-adamantylamine, as determined by GCMS and HRMS, respectively (data not shown). This is consistent with our

previous isothiocyanate insertion chemistry, where sterically demanding heterocumulenes were found to insert slowly, thereby promoting the undesired protodecarboxylation side reaction.<sup>9</sup>



All isolated benzamides were characterized by HRMS and <sup>1</sup>H and <sup>13</sup>C{<sup>1</sup>H} NMR spectroscopy (Figures S10–S21). Additionally, several benzamides (Figures S22–S24 and Table S1) were structurally characterized by X-ray crystallography (Figure 4). The crystalline amides are present as the E

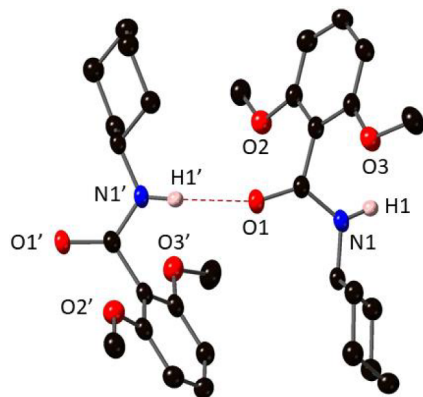


**Figure 4.** Representation (50% displacement ellipsoids) of the solid-state packing found in the X-ray crystal structure of 5-Cy. All hydrogen atoms except for the amide hydrogen are omitted for clarity. Symmetry operation used to generate atoms: (')  $1 - x, 1/2 + y, 3/2 - z$ .

conformer, affording one-dimensional polymeric chains. This is in contrast with the aggregation observed for the analogous thioamides we reported previously, where the Z conformer is exclusively observed, resulting in weakly dimeric structures due to short intermolecular N–H⋯S contacts.<sup>9</sup> In this instance, the 2,6-dimethoxy groups on the benzamide prevent rotation of the phenyl plane, resulting in a much larger N1–C1–C2–C3 torsion angle ( $-71.0(4)^\circ$ ) relative to that in *N*-cyclohexylbenzamide ( $-30.8(4)^\circ$ ).<sup>29</sup>

**Condensed-Phase Mechanistic Studies under Ligand-Free Conditions Using Stoichiometric Pd Salts.** To further probe whether the “ExIn” mechanism is operating in the condensed phase (eqs 3–5, Scheme 2), we have monitored the transformation of 2,6-dimethoxybenzoic acid to 5-Et by analyzing aliquots of reaction mixtures using <sup>1</sup>H NMR spectroscopy. The organometallic intermediate, tentatively assigned as  $[(\text{DMSO})_n\text{Pd}(\text{O}_2\text{CCF}_3)(\text{Ar})]$  (3), was generated from  $[(\text{DMSO})_n\text{Pd}(\text{O}_2\text{CCF}_3)(\text{O}_2\text{CAr})]$  (2) as previously described (Figure 5a).<sup>9,10,28</sup> Upon addition of ethyl isocyanate at room temperature, the resonance attributed to the H<sub>para</sub> proton shifts downfield by 0.16 ppm, likely due to the insertion of the isocyanate, affording an amidate complex (Figure 5b). No major chemical shift changes for these resonances were observed upon addition of formic acid (Figure 5c). In fact, these resonances (Figure 5b) are identical with those of the isolated and purified amide (Figure 5d). This indicates that the amidate complex 5-Et undergoes rapid protodemetalation in the absence of an exogenous hydrogen source. It is important to highlight that 1,3-dimethoxybenzene is only a minor side

product relative to the desired insertion product (the relative ratio is 1:25, data not shown) on the basis of a comparison of the integrated areas associated with the resonances at 6.52 ppm (due to the 4,6-protons of 1,3-dimethoxybenzene) and 6.65 ppm (due to the 3,5-protons of 5-Et) in an expanded Figure 5c.

**DFT Calculations of Elementary Steps under Ligand-Free Conditions.** The ligand-free palladium-mediated decarboxylation of *o*-methoxy-substituted benzoic acids in DMSO has been extensively studied experimentally<sup>28,30</sup> and theoretically.<sup>31,32</sup> We therefore focused specifically on the isocyanate coordination and insertion steps using DFT calculations, as our initial gas-phase model did not capture the absence of ligands and solvent molecules. Previously,<sup>10</sup> we have shown that the identity of the acid reservoir formed as a byproduct in the first step in solution (eq 2 in Scheme 2 to form either acetic acid or trifluoroacetic acid (TFA)), has an important effect on the barriers to insertion of a carbodiimide and the competitive protodecarboxylation. The presence of TFA was found to disfavor the protodecarboxylation (eqs 10 and 11) pathway relative to acetic acid, resulting in a more productive ExIn reaction.

**Insertion Reaction of Ethyl Isocyanate with the Organopalladium Intermediate.** Here we focus on the insertion of ethyl isocyanate into the Pd–C bond of the trifluoroacetate-coordinated organopalladium complex 17g, (eq 4 of Scheme 1 and Figure 6). Insertion starts with a simple associative displacement of one of the coordinating O donor atoms of the bidentate trifluoroacetate ligand by the nitrogen of the isocyanate via transition structure TS17g-18g-N to give the coordination complex 18g-N. This is followed by the migratory insertion of isocyanate into the Pd–Ar bond to afford 19g-N. An alternative pathway, involving initial coordination of the isocyanate by the oxygen atom, affords a much higher energy surface (Figure S25). The key barrier for insertion of ethyl isocyanate (TS17g-18g-N, 16.1 kcal/mol) is considerably lower than the experimentally determined barrier ( $\Delta G^\ddagger = 27$  kcal/mol) for the undesired protonation (eq 11) to give the 1,3-dimethoxybenzene protodecarboxylation side product.<sup>28</sup> This is consistent with the mild conditions under which migratory insertion of ethyl isocyanate occurs (Scheme 4) and is thus also consistent with the high selectivity for benzamide formation over protodecarboxylation (Scheme 4 and Figure 5).

**Demetalation of the Coordinated Amidate.** A key difference in the ligand-free stoichiometric one-pot ExIn synthesis of benzamides in comparison to those of thioamides and amidines is that exogenous hydrogen sources were required to release the thioamides and amidines from the metal ion. This suggests that the amidate binds less strongly to the Pd ion than the carboxylate,<sup>33</sup> whereas the thioamides and amidines bind more strongly.<sup>34</sup> Since there is a dearth of experimental thermodynamic data on binding energies of these anions to Pd centers, DFT calculations were used to investigate the overall energetics for demetalation of 19g-N and the related thioamidate and amidinate complexes by TFA to return to the starting  $[(\text{DMSO})_n\text{Pd}(\text{O}_2\text{CCF}_3)_2]$  complex (Table 4). Release of the benzamide via protonation by TFA is exergonic, while for thioamides and amidines the reactions are not thermodynamically favored. These data explain why an exogenous hydrogen source is not required to release the benzamide from the metal but is required to release related thioamides and amidines.

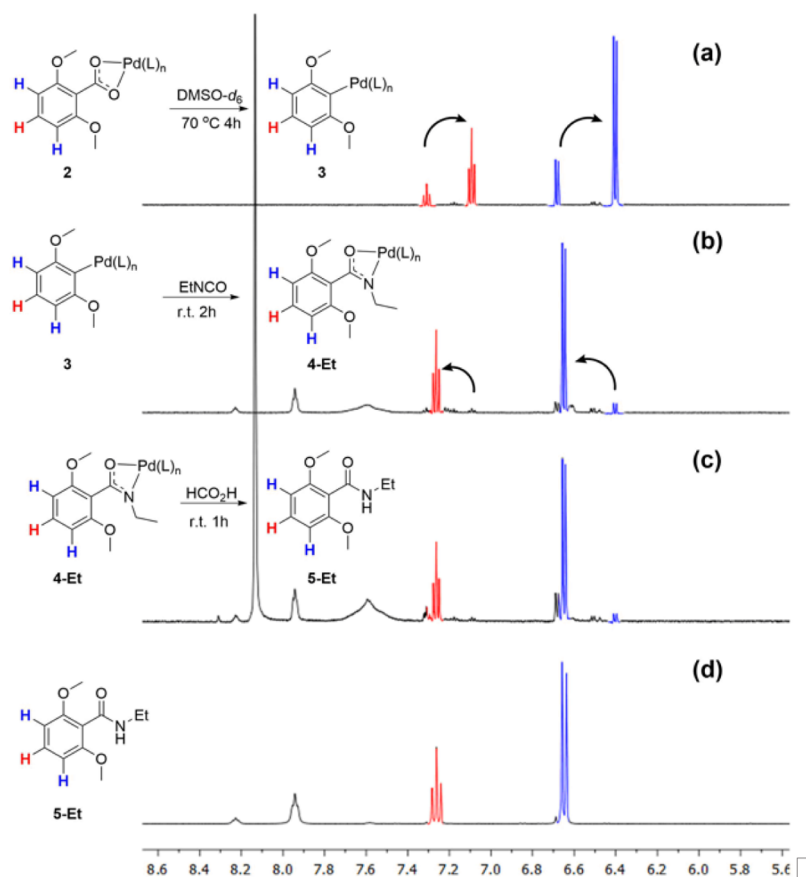


**Figure 5.** Pd(O<sub>2</sub>CCF<sub>3</sub>)<sub>2</sub>-induced transformation of 2,6-dimethoxybenzoic acid to benzamide monitored by <sup>1</sup>H NMR spectroscopy (600 MHz) in DMSO-*d*<sub>6</sub> (only the resonances due to the aromatic protons are shown): (a) decarboxylation of benzoate palladium complex for 4 h; (b) insertion of ethyl isocyanate into the Pd–C bond after 2 h; (c) addition of formic acid to the mixture; (d) purified benzamide product (5-Et) measured at 400 MHz. The arrows in (a) and (b) are used to show the change in chemical shift during the transformation.

### Solution-Phase Experiments: Palladium-Catalyzed Amide Synthesis Activated by a Microwave Reactor.

The NMR experiments indicate rapid protonation of the intermediate amidate complex in the absence of exogenous acid, suggesting the potential for this “ExIn” reaction to proceed with a catalytic quantity of Pd(O<sub>2</sub>CCF<sub>3</sub>)<sub>2</sub>. The reaction of 2,6-dimethoxybenzoic acid with cyclohexyl isocyanate in DMSO with Pd(O<sub>2</sub>CCF<sub>3</sub>)<sub>2</sub> (5 mol %) followed by microwave irradiation<sup>35</sup> at 130 °C for 30 min was investigated by <sup>1</sup>H NMR analysis of the crude reaction mixture and indicated the formation of 5-Cy in 22% yield (Table 5, entry 1). Larhed previously developed a decarboxylative Pd(O<sub>2</sub>CCF<sub>3</sub>)<sub>2</sub> catalyzed synthesis of aryl amidines from 2,4,6-trimethoxybenzoic acid and aryl trifluoroborates.<sup>36,37</sup> In that study, the combination of 6-methyl-2,2′-bipyridyl (6mbpy) as the ligand and *N*-methylpyrrolidinone (NMP) as the solvent were found to greatly enhance the product yield. Repeating the reaction in NMP with a ligand loading of 7.5% afforded 5-Cy in good yield (Table 5, entry 2). Next, we conducted a screening of solvents (Table 5). The performance of DMSO and dimethylformamide (DMF) is similar to that of NMP (Table 5, entries 3 and 4), while dimethylacetamide (DMA) and cyrene<sup>38</sup> performed poorly (Table 5, entries 5 and 6). It is noteworthy that a control experiment performed with the addition of TFA (Table 5, entry 7) afforded an inferior yield; clearly a lower concentration of TFA is crucial for a productive ExIn reaction in comparison with the protodecarboxylation side reaction (eqs 10 and 11).<sup>28,39</sup>

Having identified NMP as the solvent of choice, the effect of using different ligands was investigated (Table 6). The 6mbpy ligand used in the test reaction was found to perform the best. Symmetrically substituted bpy and phen ligands all displayed significantly inferior performance. These outcomes mirror those reported for the decarboxylative synthesis of aryl amidines.<sup>36</sup> In the current work, the main reason for the poorer performance is an increase in the formation of the 1,3-dimethoxybenzene side product (eqs 10 and 11), on the basis of the <sup>1</sup>H NMR spectra of the crude reaction mixtures (data not shown).

The use of different substituted isocyanates was also investigated (Scheme 5). Both aliphatic and aryl isocyanates afford the corresponding benzamides 5 in good yields. When 2,4,6-trimethoxybenzoic acid was employed instead of 2,6-dimethoxybenzoic acid, the corresponding benzamides 5b (Figures S26–S36 and Table S3) were obtained but in lower yields. Nonetheless, these yields are significantly better than those reported for trimethoxybenzamides developed as selective P-glycoprotein inhibitors and prepared from the reaction of the benzoic acid with thionyl chloride followed by the reaction of the resultant acid chloride with aniline.<sup>14</sup>

Previously, we observed deinsertion of phenyl isocyanate as the major fragmentation channel for ligated palladium amidate cations in the gas phase (Figure 1c). Indeed, there are several reports of the deinsertion of aryl isocyanates from a late-transition-metal benzamidate complex in solution.<sup>11,40</sup> We became intrigued as to whether protodemetalation and C–C

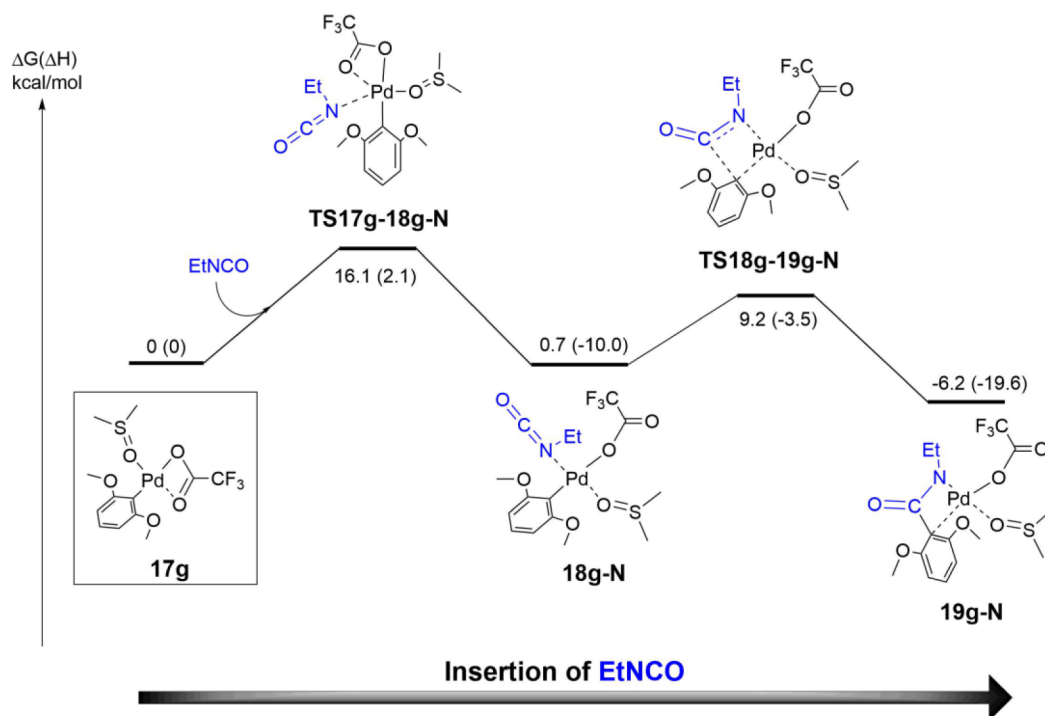
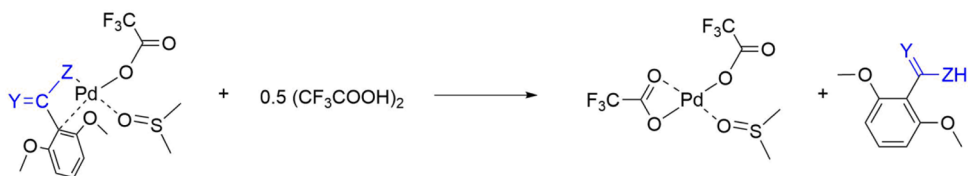


**Figure 6.** DFT calculated energy surface showing insertion of ethyl isocyanate into  $[(L)_n\text{Pd}(\text{Ar})]$  (**17g**). The relative Gibbs energies and enthalpies (in parentheses) are given in kcal/mol and were calculated at the B3LYP-D3BJ/BS2//M06/BS1 level of theory in DMSO using the CPCM approach.

**Table 4.** Calculated Gibbs Free Energies and Enthalpies for the Protodemetalation of Palladium Benzamidate, Thioamidate, and Amidinate Complexes by TFA in DMSO



system	Y	Z	$\Delta G$ (kcal/mol)	$\Delta H$ (kcal/mol)
this work	O	$\text{N}(\text{C}_2\text{H}_5)$	-1.2	5.5
ref 7	S	$\text{N}(\text{CH}_3)$	17.5	25.0
ref 9	$\text{N}(\text{CH}(\text{CH}_3)_2)$	$\text{N}(\text{CH}(\text{CH}_3)_2)$	15.9	23.5

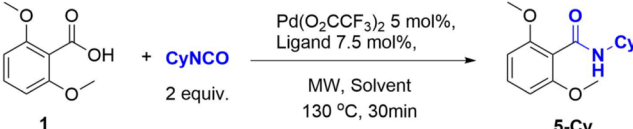
bond formation were reversible under the catalytic regime. To this end, we first performed a crossover experiment: **5-Ph** and cyclohexyl isocyanate (4 equiv) were subjected to the catalytic regime (Scheme 6). Interrogation of the reaction crude by GCMS and HRMS revealed the formation of trace amounts of **5-Cy** ( $m/z$  264.16, Figure S37a). The detection of 1-cyclohexyl-3-phenylurea further supports the extrusion of phenyl isocyanate ( $m/z$  219.15, Figure S37a). Similarly, subjecting **5-Cy** and phenyl isocyanate (4 equiv) to the catalytic regime afforded **5-Ph** ( $m/z$  258.11, Figure S37b) in ca. 5% yield on the basis of analysis by GCMS (Scheme 6) (Figure S37c). DFT calculations indicate that the free energy changes for these reactions are negligible; hence, the outcomes of these reactions signal kinetic barriers for benzamide deprotonation or isocyanate extrusion. A similar control reaction revealed that the undesired protonation of the organopalladium intermediate (eq 11) is irreversible under the catalytic regime.

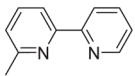
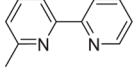
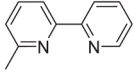
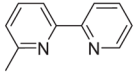
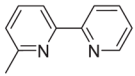
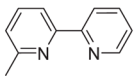
**DFT Calculations on the Competition among Insertion of Isocyanate, Protonation of Amidate Palla-**

**dium, and Protodecarboxylation of the 6-Methyl-2,2'-bipyridyl Aryl Palladium Intermediate.** The role of the ligand 6mbpy on the competing insertion and protodecarboxylation pathways (eq 3, Scheme 2) was probed by DFT calculations. We first modeled the insertion of ligated palladium complexes in the solution phase (Figure 7, right). In this instance the ground state for the reaction was found to be a four-coordinate palladium complex ligated by a molecule of NMP, **17f**. Associative substitution of the solvent molecule by ethyl isocyanate via **TS17f-18f** is rate-determining for the C–C bond formation pathway. Protodecarboxylation (Figure 7, left) proceeds through a notably higher barrier, **TS21f-22f**, which is a five-coordinate transition structure en route to the proton being delivered by the coordinated TFA.<sup>41</sup> The  $\kappa^2\text{-N,O}$ -benzamidate complex **20f** is also the slightly favored thermodynamic product.

To complete the catalytic cycle, the process of protodemetalation starting from the  $\kappa^2\text{-N,C}$ -benzamidate palladium complex **19f**<sup>42</sup> to regenerate the benzoate-coordinated palladium complex **6** was probed using DFT calculations

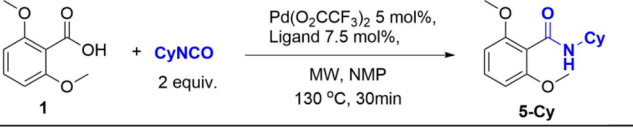
Table 5. Additive and Solvent Screening

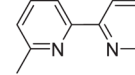
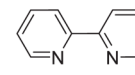
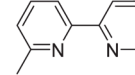
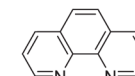
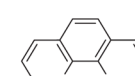


Entry	Ligand	Solvent	Yield (%) <sup>(a)</sup>
1	-	NMP	22%
2		NMP	76%
3		DMSO	79%
4		DMF	72%
5		DMA	48%
6		Cyrene	4%
7		NMP	63% <sup>(b)</sup>

<sup>a</sup>Calculated yields of product using <sup>1</sup>H NMR spectroscopic analysis with a known internal standard; <sup>b</sup>With TFA (2 equiv.).

Table 6. Ligand Screening



Entry	Ligand	Solvent	Yield (%) <sup>(a)</sup>
1		NMP	76%
2		NMP	13%
3		NMP	2%
4		NMP	18%
5		NMP	16%

<sup>a</sup>Calculated yields of product using <sup>1</sup>H NMR spectroscopic analysis with a known internal standard.

(Figure 8). The key transition state, TS24f-25f, where the proton is transferred from the TFA to the oxygen atom of the benzamidate, lies 2 kcal/mol lower than the rate-determining step on the protodecarboxylation pathway (TS21f-22f, 11.8 kcal/mol). This result is consistent with the experimental finding that isocyanate insertion and protodemetalation can

occur rapidly relative to the nonproductive protodecarboxylation pathway (eqs 10 and 11).

These mechanistic studies and our previous work allow the proposal of a plausible catalytic cycle (Figure 9). The initial benzoate complex 2 undergoes decarboxylation to afford the arylpalladium complex 3. Coordination of the isocyanate, followed by migratory insertion, forms the C–C bond and produces the key benzamidate intermediate 4'. Subsequent protodemetalation by benzoic acid, mediated by trifluoroacetate, releases the benzamide and closes the catalytic cycle.

## CONCLUSIONS

We have used a mechanistic-based approach that blends fundamental gas-phase ion chemistry, condensed-phase stoichiometric reactions, and DFT calculations to study the palladium-mediated conversion of aromatic carboxylic acids to benzamides via the isohypsic “ExIn” reaction sequence. A key finding is that protodemetalation of the benzamidate intermediate is thermodynamically favorable in comparison to previous “ExIn” systems where an exogenous hydrogen source was needed to release the product from the metal. These fundamental studies enabled a microwave irradiation assisted protocol to be developed, which affords *o*-methoxy-substituted benzamides in moderate to good yields, employing catalytic amounts of palladium(II). This approach represents a significant improvement on the current methods to prepare *o*-methoxy-substituted benzamides, which either are low yielding or suffer poor atom economy. We are currently exploring the use of other metals and ligands to extend the scope of amide synthesis via ExIn reactions to include a wider range of aromatic carboxylic acids.

## EXPERIMENTAL METHODS

**Gas-Phase Experiments. Sample Preparation.** The gas-phase collision-induced dissociation (CID) of [(L)Pd(O<sub>2</sub>CR)]<sup>+</sup> to form [(L)Pd(R)]<sup>+</sup> and subsequent ion–molecule reaction studies were conducted in a similar manner to those reported for the reactivity studies of [(phen)M(CH<sub>3</sub>)]<sup>+</sup>.<sup>43–45</sup> For example, 10 μL of methanolic solutions of palladium salt (5 mM), benzoic acid (10 mM), and ligand (10 mM) were mixed and then diluted to a final concentration of 0.05 mM in metal. The solution was transferred via syringe pump operating at 5 μL min<sup>-1</sup> to the electrospray ionization source of a Thermo Finnigan LTQ-ESI mass spectrometer previously modified to allow the introduction of neutral reagents into the ion trap.<sup>46,47</sup> Data were collected with three microscans and between 20 and 100 duplicate spectra.

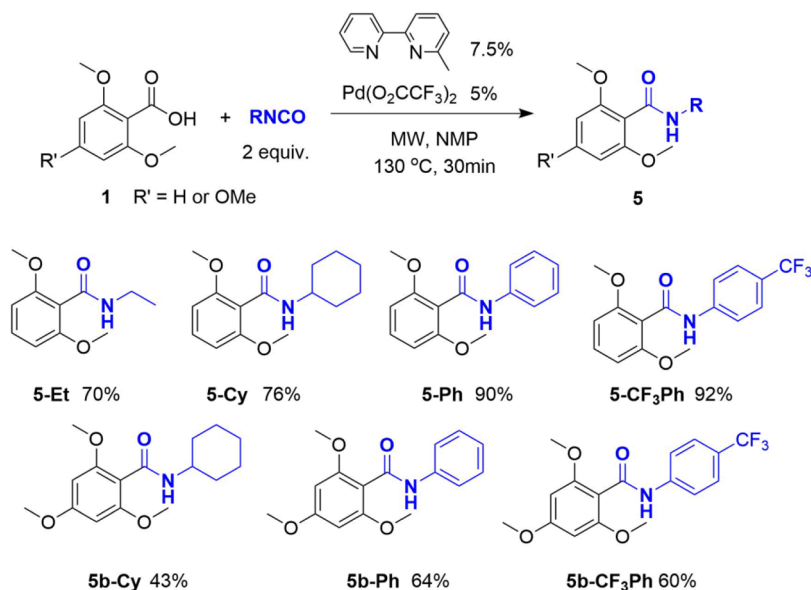
**Mass Spectrometry Source Conditions.** Typical electrospray source conditions were as follows.

**Collision-induced dissociation (CID):** sheath gas, 10 arbitrary units; auxiliary gas, 5 arbitrary units; sweep gas, 0 arbitrary units; spray voltage, 4 kV; capillary temperature, 250 °C; capillary voltage, 2 V; tube lens voltage, 75 V. The precursor ion was mass-selected with a window of 1 *m/z*, and collision-induced dissociation was carried out using the helium bath gas by activating the ion with an activation time of 30 ms. A normalized collision energy (NCE) was chosen to deplete the precursor ion to 10%.

**Ion–molecule reaction (IMR):** sheath gas, 10 arbitrary units; auxiliary gas, 5 arbitrary units; sweep gas, 0 arbitrary units; spray voltage, 4 kV; capillary temperature, 250 °C; capillary voltage, 2 V; tube lens voltage, 75 V.

**Solution-Phase Experiments. General Methods.** Unless otherwise stated, all reagents were purchased from commercial sources and used without further purification. Flash column chromatography was carried out using Davisil Chromatographic Silica Media (40–63 μm, with solvent systems as specified) at the stationary phase.

## Scheme 5. Scope of the “ExIn” Reaction with Regard to the Isocyanates and Substituted Benzoic Acids



## Scheme 6. Reversibility of Protodemetalation and C–C Bond Formation

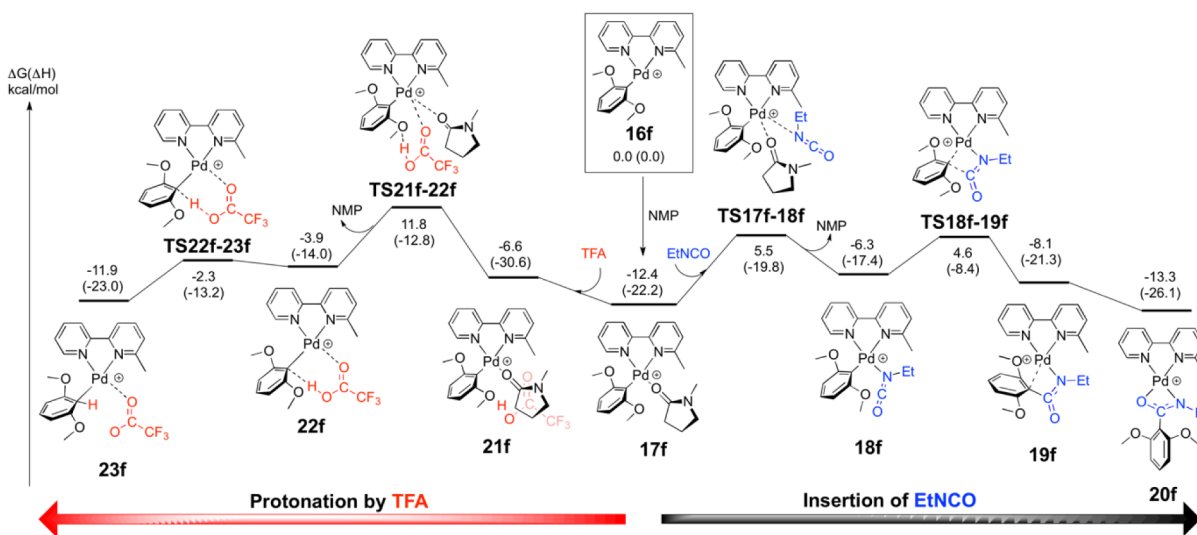
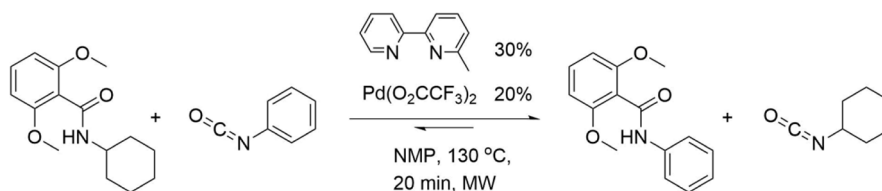


**Figure 7.** DFT calculated energy surface showing protonation (left) and insertion (right) of ethyl isocyanate into  $[(6\text{Meppy})\text{Pd}(\text{Ar})]^+$  (**16f**). The relative Gibbs energies and enthalpies (in parentheses) are given in kcal/mol and were calculated at the B3LYP-D3BJ/BS2//M06/BS1 level of theory in DMA using the CPCM approach.

<sup>1</sup>H NMR and <sup>13</sup>C{<sup>1</sup>H} NMR spectra were recorded either on a 600 MHz Varian/Agilent 600-MR or 400 MHz Varian/INOVA 400-AR spectrometer at 298 K. Chemical shifts are reported in parts per million (ppm) and referenced to the residual solvent peak (DMSO-*d*<sub>6</sub>: <sup>1</sup>H NMR 2.50 ppm, <sup>13</sup>C NMR 39.52 ppm). Coupling constants (*J*) are reported in Hertz (Hz). Standard abbreviations indicating multiplicity were used as follows: m = multiplet, quint = quintet, q = quartet, t = triplet, d = doublet, s = singlet, br = broad. High-resolution electrospray ionization mass spectra (ESI- HRMS) were

collected on a Thermo Scientific Exactive Plus Orbitrap mass spectrometer (Thermo, Bremen, Germany).

**<sup>1</sup>H NMR Monitoring Experiment.** A round-bottom flask was charged with 2,6-dimethoxybenzoic acid (0.2 mmol) and palladium(II) trifluoroacetate (0.22 mmol) under N<sub>2</sub>. DMSO-*d*<sub>6</sub> (2 mL) was added under N<sub>2</sub>, and the mixture was stirred for 5 min at room temperature. For all sequential <sup>1</sup>H NMR experiments used to monitor reaction outcomes, a 50 μL aliquot of the reaction mixture was withdrawn from the sample tube, transferred to an NMR tube, and

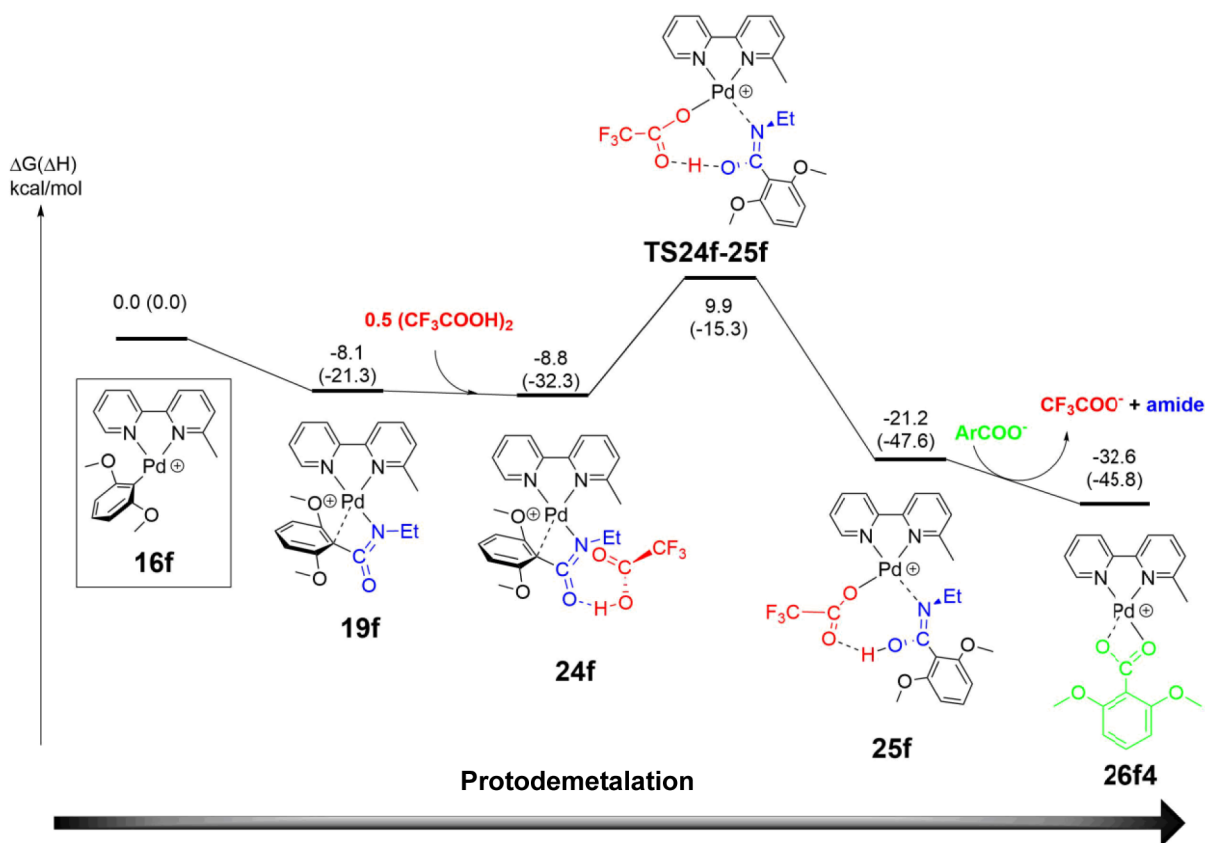


**Figure 8.** DFT calculated energy surface showing protonation of  $[(6\text{Meppy})\text{Pd}(\text{NEtC}(\text{O})\text{Ar})]^+$ . The relative Gibbs energies and enthalpies (in parentheses) are given in kcal/mol and were calculated at the B3LYP-D3BJ/BS2//M06/BS1 level of theory in DMA using the CPCM approach.

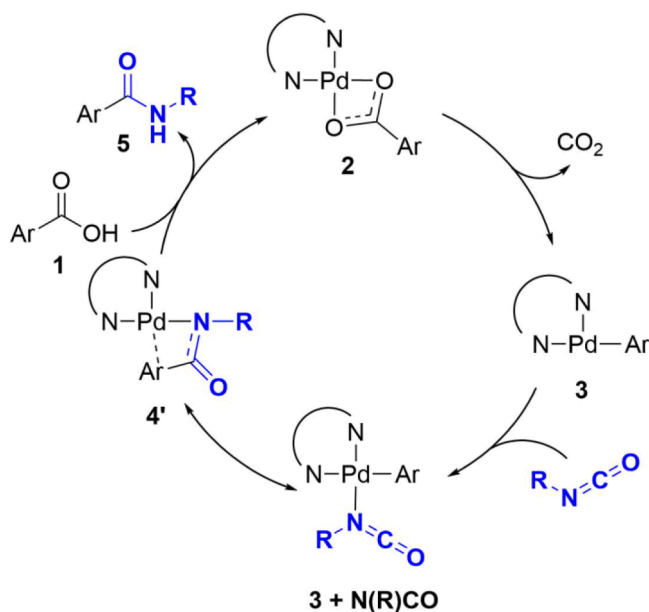


**Figure 9.** Proposed catalytic cycle for the decarboxylative synthesis of benzamides.

diluted with 600  $\mu\text{L}$  of DMSO- $d_6$  and then a  $^1\text{H}$  NMR spectrum was collected. The mixture was then warmed to 70  $^\circ\text{C}$  for 4 h.  $^1\text{H}$  NMR spectra were recorded hourly, and the formation of an aryl palladium species was confirmed by the appearance of a new upfield-shifted set of aromatic peaks. The mixture was cooled to room temperature. Ethyl isocyanate (2 equiv) was added, and then a  $^1\text{H}$  NMR spectrum was collected hourly until the aryl palladium intermediate was

completely consumed. Formic acid (10 equiv) was then added to the solution and stirred for a further 1 h at room temperature. A final  $^1\text{H}$  NMR spectrum of the reaction mixture was recorded. The recorded spectra were stacked, including the spectrum of pure product, and are shown in Figure 5. ESI/HRMS analyses was conducted on the final NMR sample by diluting in methanol.

**General Experimental Procedures in the Solution Phase.**  
**One-Pot Synthesis Using Ligand-Free Stoichiometric Palladium(II) Trifluoroacetate.** To a solution of 2,6-dimethoxybenzoic acid (0.5 mmol, 1 equiv) in DMSO (5 mL) was added palladium(II) trifluoroacetate (0.55 mmol, 1.1 equiv). The mixture was heated under N<sub>2</sub> at 70  $^\circ\text{C}$  for 4 h and then cooled to room temperature. RNCO (1 mmol, 2.0 equiv) was added, and the mixture was then stirred for 2 h at room temperature. Formic acid (5 mmol, 10 equiv) was then added and the reaction mixture was stirred for an additional 1 h at room temperature. Methanol (5 mL) was added to the mixture followed by water (100 mL), and the aqueous layer was extracted with ethyl acetate (3  $\times$  50 mL). The combined organic fractions were washed with water (100 mL) and brine (100 mL) and dried over anhydrous Na<sub>2</sub>SO<sub>4</sub>. The solvent was removed using a rotary evaporator, and the residue was purified by column chromatography to give amides 5.

**Microwave Method Using Catalytic Loading of Palladium(II) Trifluoroacetate with the 6-Methyl-2,2'-bipyridyl Ligand.** Palladium(II) trifluoroacetate (0.025 mmol, 5 mol %), 6-methyl-2,2'-bipyridyl (0.0375 mmol, 7.5 mol %), and NMP (1.5 mL) were placed in a 0.5–2 mL process vial, and the mixture was stirred for 2 min before 2,6-dimethoxybenzoic acid or 2,4,6-trimethoxybenzoic acid (0.5 mmol, 1 equiv) and isocyanate (1.0 mmol, 2 equiv) were added. The vial was instantly capped under air and then heated by using microwave irradiation at 130  $^\circ\text{C}$  for 30 min. Methanol (5 mL) was added to the mixture followed by water (100 mL), and the aqueous layer was extracted with ethyl acetate (3  $\times$  50 mL). The combined organic layers were washed with water (100 mL) and brine

(100 mL) and dried over anhydrous  $\text{Na}_2\text{SO}_4$ . The solvent was removed using a rotary evaporator, and the residue was purified by column chromatography to give the benzamides **5**.

**N-Ethyl-2,6-dimethoxybenzamide (5-Et)**. This compound was prepared using both the one-pot method and microwave method: yield 53 mg (51%) white solid for the one-pot method; 73 mg (70%) for the microwave method. Column chromatography (silica gel, methanol/DCM 1/50).  $^1\text{H}$  NMR (400 MHz,  $\text{DMSO}-d_6$ ):  $\delta$  7.92 (t,  $J$  = 5.6 Hz, 1H), 7.24 (t, 1H), 6.63 (d,  $J$  = 8.3 Hz, 2H), 3.70 (t, 6H) 3.17–3.10 (m, 2H), 1.03 (s, 3H).  $^{13}\text{C}\{^1\text{H}\}$  NMR (100 MHz,  $\text{DMSO}-d_6$ ):  $\delta$  164.60, 157.11, 130.17, 117.63, 104.64, 56.14, 34.03, 15.04. HR-ESMS (ESI):  $m/z$   $[\text{M} + \text{H}]^+$  calcd for  $\text{C}_{15}\text{H}_{21}\text{NO}_3$  210.11247, found 210.11257.

**N-Cyclohexyl-2,6-dimethoxybenzamide (5-Cy)**. This compound was prepared using both the one-pot method and microwave method: yield 105 mg (80%) white solid for the one-pot method; 100 mg (76%) for the microwave method. Column chromatography (silica gel, methanol/DCM 1/50).  $^1\text{H}$  NMR (400 MHz,  $\text{DMSO}-d_6$ ):  $\delta$  7.80 (d,  $J$  = 8.1 Hz, 1H), 7.23 (t,  $J$  = 8.3 Hz, 1H), 6.62 (d,  $J$  = 8.4 Hz, 2H), 3.69 (s, 6H), 3.62 (dt,  $J$  = 7.0, 3.2 Hz, 1H), 1.77–1.51 (m, 5H), 1.27–1.07 (m, 5H).  $^{13}\text{C}\{^1\text{H}\}$  NMR (100 MHz,  $\text{DMSO}-d_6$ ):  $\delta$  164.13, 157.11, 130.19, 117.62, 104.71, 56.19, 48.29, 32.68, 25.68, 25.05. HR-ESMS (ESI):  $m/z$   $[\text{M} + \text{H}]^+$  calcd for  $\text{C}_{15}\text{H}_{21}\text{NO}_3$  264.15942, found 264.15905.

**N-Phenyl-2,6-dimethoxybenzamide (5-Ph)**. This compound was prepared using both the one-pot method and microwave method: yield 100 mg (78%) white solid for the one-pot method; 116 mg (90%) for the microwave method. Column chromatography (silica gel, ethyl acetate/petroleum ether 1/3), white solid (100 mg, 78%).  $^1\text{H}$  NMR (400 MHz,  $\text{DMSO}-d_6$ ):  $\delta$  10.14 (s, 1H), 7.67 (d, 2H), 7.31 (t,  $J$  = 8.4 Hz, 1H), 7.26 (t,  $J$  = 7.9 Hz, 2H), 7.01 (t,  $J$  = 7.4 Hz, 1H), 6.69 (d,  $J$  = 8.4 Hz, 2H), 3.72 (s, 6H).  $^{13}\text{C}\{^1\text{H}\}$  NMR (100 MHz,  $\text{DMSO}-d_6$ ):  $\delta$  163.77, 157.15, 140.12, 130.78, 129.06, 123.51, 119.35, 117.35, 104.69, 56.22. HR-ESMS (ESI):  $m/z$   $[\text{M} + \text{H}]^+$  calcd for  $\text{C}_{15}\text{H}_{21}\text{NO}_3$  258.11247, found 258.11215. Spectroscopic data are consistent with the literature reported data.<sup>9</sup>

**N-(4-(Trifluoromethyl)phenyl)-2,6-dimethoxybenzamide (5-CF<sub>3</sub>Ph)**. This compound was prepared using both the one-pot method and microwave method: yield 109 mg (67%) white solid for the one-pot method; 149 mg (92%) for the microwave method. Column chromatography (silica gel, ethyl acetate/petroleum ether 1/3).  $^1\text{H}$  NMR (400 MHz,  $\text{DMSO}-d_6$ ):  $\delta$  10.56 (s, 1H), 7.88 (d,  $J$  = 8.5 Hz, 2H), 7.65 (d,  $J$  = 8.6 Hz, 2H), 7.35 (t,  $J$  = 8.4 Hz, 1H), 6.73 (d,  $J$  = 8.4 Hz, 2H), 3.74 (s, 6H).  $^{13}\text{C}\{^1\text{H}\}$  NMR (100 MHz,  $\text{DMSO}-d_6$ ):  $\delta$  164.47, 157.17, 143.50, 131.16, 126.49, 126.45, 123.78, 119.30, 118.57, 116.76, 104.72, 56.28. HR-ESMS (ESI):  $m/z$   $[\text{M} + \text{H}]^+$  calcd for  $\text{C}_{15}\text{H}_{21}\text{NO}_3$  326.09985, found 326.09994.

**N-Cyclohexyl-2,4,6-trimethoxybenzamide (5b-Cy)**. This compound was prepared using the microwave method: yield 63 mg (43%) as a white solid. Column chromatography (silica gel, methanol/DCM 1/50).  $^1\text{H}$  NMR (400 MHz,  $\text{DMSO}-d_6$ ):  $\delta$  7.66 (d,  $J$  = 8.1 Hz, 1H), 6.18 (s, 2H), 3.75 (s, 3H), 3.68 (s, 6H), 3.60 (dt,  $J$  = 7.0, 3.2 Hz, 1H), 1.72–1.47 (m, 5H), 1.22–1.03 (m, 5H).  $^{13}\text{C}\{^1\text{H}\}$  NMR (100 MHz,  $\text{DMSO}-d_6$ ):  $\delta$  163.92, 161.41, 158.01, 157.05, 91.32, 56.16, 55.83, 48.24, 33.80, 32.74, 25.77, 25.09. HR-ESMS (ESI):  $m/z$   $[\text{M} + \text{H}]^+$  calcd for  $\text{C}_{15}\text{H}_{21}\text{NO}_3$  294.16998, found 294.16957.

**N-Phenyl-2,4,6-trimethoxybenzamide (5b-Ph)**. This compound was prepared using the microwave method: yield 92 mg (64%) as a white solid. Column chromatography (silica gel, ethyl acetate/petroleum ether 1/3).  $^1\text{H}$  NMR (400 MHz, chloroform-*d*):  $\delta$  7.64 (d,  $J$  = 7.9 Hz, 2H), 7.52 (s, 1H), 7.33 (t,  $J$  = 7.8 Hz, 2H), 7.10 (t,  $J$  = 7.4 Hz, 1H), 6.14 (s, 2H), 3.84 (s, 3H), 3.82 (s, 6H).  $^{13}\text{C}\{^1\text{H}\}$  NMR (100 MHz, chloroform-*d*):  $\delta$  163.54, 162.44, 158.85, 138.54, 128.90, 123.92, 119.55, 109.01, 90.76, 56.03, 55.45. HR-ESMS (ESI):  $m/z$   $[\text{M} + \text{H}]^+$  calcd for  $\text{C}_{15}\text{H}_{21}\text{NO}_3$  288.12303, found 288.12296.

**N-(4-(Trifluoromethyl)phenyl)-2,4,6-trimethoxybenzamide (5b-CF<sub>3</sub>Ph)**. This compound was prepared using the microwave method: yield 106 mg (60%) as a white solid; Column chromatography (silica gel, ethyl acetate/petroleum ether = 1:3);  $^1\text{H}$  NMR (400 MHz,

$\text{DMSO}-d_6$ ):  $\delta$  10.45 (s, 1H), 7.88 (d,  $J$  = 8.4 Hz, 2H), 7.64 (d,  $J$  = 8.5 Hz, 2H), 6.28 (s, 2H), 3.80 (s, 3H), 3.73 (s, 6H).  $^{13}\text{C}\{^1\text{H}\}$  NMR (100 MHz,  $\text{DMSO}-d_6$ ):  $\delta$  164.45, 162.24, 158.17, 143.67, 126.40, 123.62, 123.31, 119.20, 109.98, 91.29, 56.25, 56.00. HR-ESMS (ESI):  $m/z$   $[\text{M} + \text{H}]^+$  calcd for  $\text{C}_{15}\text{H}_{21}\text{NO}_3$  356.11042, found 356.11085.

**X-ray Crystallography.** Single-crystal X-ray diffraction data for all samples were collected as follows: a typical crystal was mounted on a MiTeGen Micromount using high-viscosity oil and cooled rapidly to 100(2) K under a stream of nitrogen gas using an Oxford Cryostream cooling device. Diffraction data were collected ( $\omega$  scans) on a Rigaku XtaLAB Synergy or Synergy-S diffractometer equipped with a HyPix detector using  $\text{Cu K}\alpha$  radiation ( $\lambda$  = 1.54184 Å). Raw frame data were reduced using CrysAlisPro. The structures were solved using SHELXT,<sup>48</sup> and the refinement was carried out with SHELXL (version 2018/3)<sup>49</sup> employing full-matrix least squares on  $F^2$  using the OLEX2 software packages.<sup>50</sup> All non-hydrogen atoms were refined anisotropically. The hydrogen atoms were placed in geometrically calculated positions and refined using a riding model. Selected crystallographic data and comments about individual crystal structures can be found in the Supporting Information.

**DFT Calculations.** Gaussian 09<sup>51</sup> was used to fully optimize all structures at the M06 level of density functional theory (DFT).<sup>52</sup> The effective-core potential of Hay and Wadt with a double- $\xi$  valence basis set (LANL2DZ) was chosen to describe Pd.<sup>53,54</sup> The 6-31G(d) basis set was used for other atoms.<sup>55</sup> A polarization function of  $\xi f$  = 1.472 was also added for Pd.<sup>56,57</sup> This basis set combination will be referred to as BS1. Solvation effects of DMSO on the optimized structures were accounted for using the CPCM model.<sup>58</sup> Frequency calculations were carried out at the same level of theory as those for the structural optimization. Transition structures were located using the Berny algorithm. Intrinsic reaction coordinate (IRC) calculations were used to confirm the connectivity between transition structures and minima.

To further refine the energies obtained from the M06/BS1 calculations, we carried out single-point energy calculations for all of the structures with a larger basis set (BS2) at the B3LYP-D3BJ level of theory.<sup>59–62</sup> BS2 utilizes def2-TZVP11 for all atoms along with the effective core potential including scalar relativistic effects for Pd.<sup>63</sup> The solvent effect using the CPCM approach was considered for the DMSO or DMF (as an analogue of NMP) system in the single-point calculations. The B3LYP-D3BJ calculations were used to overcome the deficiency of the M06 level in incorporating long-range correlation for dispersion forces. To estimate the corresponding enthalpy,  $\Delta H$ , and Gibbs energies,  $\Delta G$ , the corrections were calculated at the M06/BS1 levels and finally added to the corresponding single-point energies. Entropy calculations for the solvent system were adjusted by the method proposed by Okuno.<sup>64</sup> An additional correction was made to account for the fact that DMSO or NMP participates in the equilibrium. Thus, when the energy profiles for Figures 6–8 were calculated, the concentration of the solvent was set using the method of Keith and Carter (we utilized eq 6 of their paper).<sup>65</sup> We have used the corrected enthalpy and Gibbs free energies obtained from the B3LYP-D3BJ/BS2//M06/BS1 calculations throughout unless otherwise stated.

## ■ ASSOCIATED CONTENT

### Supporting Information

The Supporting Information is available free of charge at <https://pubs.acs.org/doi/10.1021/acs.organomet.9b00820>.

Tables of DFT calculated thermochemistry for transformation of aromatic carboxylic acids into amidines, mass spectra showing decarboxylation and fragmentation reactions of adducts of organopalladium cations and isocyanates,  $^1\text{H}$  and  $^{13}\text{C}\{^1\text{H}\}$  NMR and HRMS spectra of all isolated benzamides, discussion of crystallographic studies, tables for crystal data and structure refinement (PDF)

Cartesian coordinates for the calculated structures (XYZ)

## Accession Codes

CCDC 1937864–1937866 and 1966555–1966557 contain the supplementary crystallographic data for this paper. These data can be obtained free of charge via [www.ccdc.cam.ac.uk/data\\_request/cif](http://www.ccdc.cam.ac.uk/data_request/cif), or by emailing [data\\_request@ccdc.cam.ac.uk](mailto:data_request@ccdc.cam.ac.uk), or by contacting The Cambridge Crystallographic Data Centre, 12 Union Road, Cambridge CB2 1EZ, UK; fax: +44 1223 336033.

## AUTHOR INFORMATION

### Corresponding Author

Richard A. J. O'Hair – School of Chemistry, Bio21 Institute of Molecular Science and Biotechnology, The University of Melbourne, Parkville 3010, Australia; [orcid.org/0000-0002-8044-0502](https://orcid.org/0000-0002-8044-0502); Phone: +613 8344-2452; Email: [rohair@unimelb.edu.au](mailto:rohair@unimelb.edu.au); Fax: +613 9347-5180

### Authors

Yang Yang – School of Chemistry, Bio21 Institute of Molecular Science and Biotechnology, The University of Melbourne, Parkville 3010, Australia

Allan J. Canty – School of Natural Sciences-Chemistry, University of Tasmania, Hobart 7001, Australia; [orcid.org/0000-0003-4091-6040](https://orcid.org/0000-0003-4091-6040)

Alasdair I. McKay – School of Chemistry, Bio21 Institute of Molecular Science and Biotechnology, The University of Melbourne, Parkville 3010, Australia

Paul S. Donnelly – School of Chemistry, Bio21 Institute of Molecular Science and Biotechnology, The University of Melbourne, Parkville 3010, Australia; [orcid.org/0000-0001-5373-0080](https://orcid.org/0000-0001-5373-0080)

Complete contact information is available at: <https://pubs.acs.org/10.1021/acs.organomet.9b00820>

### Notes

The authors declare no competing financial interest.

## ACKNOWLEDGMENTS

We acknowledge the support of the ARC (DP180101187 funding to A.J.C., P.S.D., and R.A.J.O.), and the National Computing Infrastructure. The Thermo Orbitrap Fusion Lumos mass spectrometer was accessed via the Bio21 Mass Spectrometry and Proteomics Facility with thanks. The single-crystal X-ray diffractometers used in this study were funded by the ARC (LE170100065).

## REFERENCES

- (1) Montalbetti, C. A. G. N.; Falque, V. Amide bond formation and peptide coupling. *Tetrahedron* **2005**, *61*, 10827–10852.
- (2) de Figueiredo, R. M.; Suppo, J.-S.; Campagne, J.-M. Nonclassical Routes for Amide Bond Formation. *Chem. Rev.* **2016**, *116*, 12029–12122.
- (3) El-Faham, A.; Albericio, F. Peptide Coupling Reagents, More than a Letter Soup. *Chem. Rev.* **2011**, *111*, 6557–6602.
- (4) Pattabiraman, V. R.; Bode, J. W. Rethinking amide bond synthesis. *Nature* **2011**, *480*, 471–479.
- (5) An emerging problem with these coupling agents is that repeated exposure to them can lead to health problems including anaphylaxis, see: McKnelly, K. J.; Sokol, W.; Nowick, J. S. Anaphylaxis Induced by Peptide Coupling Agents: Lessons Learned from Repeated Exposure to HATU, HBTU, and HCTU. *J. Org. Chem.* **2019**, DOI: [10.1021/acs.joc.9b03280](https://doi.org/10.1021/acs.joc.9b03280).

- (6) Lew, T. T. S.; Lim, D. S. W.; Zhang, Y. Copper(i)-catalyzed amidation reaction of organoboronic esters and isocyanates. *Green Chem.* **2015**, *17*, 5140–5143.

- (7) Yu, X.; Wang, D.-S.; Xu, Z.; Yang, B.; Wang, D. The synthesis of unsymmetric diamides through Rh-catalyzed selective C-H bond activation of amides with isocyanates. *Org. Chem. Front.* **2017**, *4*, 1011–1018.

- (8) McKay, A. I.; Altalhi, W. A. O.; McInnes, L. E.; Czyz, M. L.; Canty, A. J.; Donnelly, P. S.; O'Hair, R. A. J. Identification of the Side Products that Diminish the Yields of the Monoamidated Product in Metal-Catalyzed C-H Amidation of 2-Phenylpyridine with Arylisocyanates. *J. Org. Chem.* **2020**, DOI: [10.1021/acs.joc.9b02831](https://doi.org/10.1021/acs.joc.9b02831).

- (9) Noor, A.; Li, J.; Khairallah, G. N.; Li, Z.; Ghari, H.; Canty, A. J.; Ariaifard, A.; Donnelly, P. S.; O'Hair, R. A. J. A one-pot route to thioamides discovered by gas-phase studies: palladium-mediated CO<sub>2</sub> extrusion followed by insertion of isothiocyanates. *Chem. Commun.* **2017**, *53*, 3854–3857.

- (10) Yang, Y.; Noor, A.; Canty, A. J.; Ariaifard, A.; Donnelly, P. S.; O'Hair, R. A. J. Synthesis of Amidines by Palladium-Mediated CO<sub>2</sub> Extrusion Followed by Insertion of Carbodiimides: Translating Mechanistic Studies to Develop a One-Pot Method. *Organometallics* **2019**, *38*, 424–435.

- (11) Moselage, M.; Li, J.; Kramm, F.; Ackermann, L. Ruthenium-(II)-Catalyzed C-C Arylations and Alkylations: Decarbonylative C-C Functionalizations. *Angew. Chem., Int. Ed.* **2017**, *56*, 5341–5344.

- (12) Myers, A. G.; Tanaka, D.; Mannion, M. R. Development of a Decarboxylative Palladation Reaction and Its Use in a Heck-type Olefination of Arene Carboxylates. *J. Am. Chem. Soc.* **2002**, *124*, 11250–11251.

- (13) Dickstein, J. S.; Mulrooney, C. A.; O'Brien, E. M.; Morgan, B. J.; Kozlowski, M. C. Development of a Catalytic Aromatic Decarboxylation Reaction. *Org. Lett.* **2007**, *9*, 2441–2444.

- (14) Stefanachi, A.; Mangiatordi, G. F.; Tardia, P.; Alberga, D.; Leonetti, F.; Niso, M.; Colabufo, N. A.; Adamo, C.; Nicolotti, O.; Cellamare, S. Design, synthesis, biological evaluation, NMR and DFT studies of structurally simplified trimethoxy benzamides as selective P-glycoprotein inhibitors: the role of molecular flatness. *Chem. Biol. Drug Des.* **2016**, *88*, 820–831.

- (15) There is a surprising lack of known heats of formation of aromatic amides. Using the following gas-phase heats of formation, eq 1 is predicted to be exothermic by 22.7 kcal/mol for the transformation of benzoic acid to benzamide:  $\Delta_f H(\text{PhCO}_2\text{H}) = -70.3$  kcal/mol;  $\Delta_f H(\text{HNCO}) = -25$  kcal/mol;  $\Delta_f H(\text{PhC}(\text{O})\text{NH}_2) = -24$  kcal/mol;  $\Delta_f H(\text{CO}_2) = -94$  kcal/mol. Data are from: Lias, S. G.; Bartmess, J. E.; Liebman, J. F.; Holmes, J. L.; Levin, R. D.; Mallard, W. G., Gas-Phase Ion and Neutral Thermochemistry, *J. Phys. Chem. Ref. Data* **1988**, *17*, Supplement 1.

- (16) Rodriguez, N.; Goossen, L. J. Decarboxylative coupling reactions: a modern strategy for C-C-bond formation. *Chem. Soc. Rev.* **2011**, *40*, 5030–5048.

- (17) Goossen, L. J.; Rodriguez, N.; Goossen, K. Carboxylic acids as substrates in homogeneous catalysis. *Angew. Chem., Int. Ed.* **2008**, *47*, 3100–3120.

- (18) Drover, M. W.; Love, J. A.; Schafer, L. L. 1,3-N, O-Complexes of late transition metals. Ligands with flexible bonding modes and reaction profiles. *Chem. Soc. Rev.* **2017**, *46*, 2913–2940.

- (19) Serrano, E.; Martin, R. Forging Amides Through Metal-Catalyzed C-C Coupling with Isocyanates. *Eur. J. Org. Chem.* **2018**, 3051–3064.

- (20) Pace, V.; Monticelli, S.; de la Vega-Hernández, K.; Castoldi, L. Isocyanates and isothiocyanates as versatile platforms for accessing (thio)amide-type compounds. *Org. Biomol. Chem.* **2016**, *14*, 7848–7854.

- (21) Butschke, B.; Schwarz, H. “Rollover” cyclometalation - early history, recent developments, mechanistic insights and application aspects. *Chem. Sci.* **2012**, *3*, 308–326.

- (22) Leist, M.; Kerner, C.; Ghoochany, L. T.; Farsadpour, S.; Fizia, A.; Neu, J. P.; Schön, F.; Sun, Y.; Oelkers, B.; Lang, J.; Menges, F.; Niedner-Schatteburg, G.; Salih, K. S. M.; Thiel, W. R. Roll-over

cyclometalation: A versatile tool to enhance the catalytic activity of transition metal complexes. *J. Organomet. Chem.* **2018**, *863*, 30–43.

(23) Perry, G. J. P.; Larrosa, I. Recent Progress in Decarboxylative Oxidative Cross-Coupling for Biaryl Synthesis. *Eur. J. Org. Chem.* **2017**, 3517–3527.

(24) Zhu, L.; Le, L.; Yan, M.; Au, C. T.; Qiu, R.; Kambe, N. Carbon-Carbon Bond Formation of Trifluoroacetyl Amides with Grignard Reagents via C(O)-CF<sub>3</sub> Bond Cleavage. *J. Org. Chem.* **2019**, *84*, 5635–5644.

(25) Fujita, K.-i.; Yamashita, M.; Puschmann, F.; Alvarez-Falcon, M. M.; Incarvito, C. D.; Hartwig, J. F. Organometallic Chemistry of Amidate Complexes. Accelerating Effect of Bidentate Ligands on the Reductive Elimination of N-Aryl Amidates from Palladium(II). *J. Am. Chem. Soc.* **2006**, *128*, 9044–9045.

(26) Beattie, D. D.; Bowes, E. G.; Drover, M. W.; Love, J. A.; Schafer, L. L. Oxidation State Dependent Coordination Modes: Accessing an Amidate-Supported Nickel(I)  $\delta$ -bis(C-H) Agostic Complex. *Angew. Chem., Int. Ed.* **2016**, *55*, 13290–13295.

(27) Palladium(II) complexes react with isocyanates to form coordinated ureas among other products. For leading references, see: (a) Paul, F.; Fischer, J.; Ochsenbein, P.; Osborn, J. A. Syntheses, interconversions and reactivity of heteropalladacycles made from aryl isocyanates and various phenanthroline Pd(II) precursors with small molecules. *C. R. Chim.* **2002**, *5*, 267–287. (b) Moulin, S.; Pellerin, O.; Toupet, L.; Paul, F. Formation of six-membered palladacycles from phenanthroline Pd(II) bisacetate precursors and phenylisocyanate. *C. R. Chim.* **2014**, *17*, 521–525.

(28) Dickstein, J. S.; Curto, J. M.; Gutierrez, O.; Mulrooney, C. A.; Kozlowski, M. C. Mild Aromatic Palladium-Catalyzed Protodecarboxylation: Kinetic Assessment of the Decarboxylative Palladation and the Protodepalladation Steps. *J. Org. Chem.* **2013**, *78*, 4744–4761.

(29) Khan, I. U.; Javaid, R.; Sharif, S.; Tiekink, E. R. T. N-Cyclohexylbenzamide. *Acta Crystallogr., Sect. E: Struct. Rep. Online* **2010**, *E66*, No. o1687.

(30) Tanaka, D.; Romeril, S. P.; Myers, A. G. On the Mechanism of the Palladium(II)-Catalyzed Decarboxylative Olefination of Arene Carboxylic Acids. Crystallographic Characterization of Non-Phosphine Palladium(II) Intermediates and Observation of Their Stepwise Transformation in Heck-like Processes. *J. Am. Chem. Soc.* **2005**, *127*, 10323–10333.

(31) Zhang, S.-L.; Fu, Y.; Shang, R.; Guo, Q.-X.; Liu, L. Theoretical Analysis of Factors Controlling Pd-Catalyzed Decarboxylative Coupling of Carboxylic Acids with Olefins. *J. Am. Chem. Soc.* **2010**, *132*, 638–646.

(32) Xue, L.; Su, W.; Lin, Z. A DFT study on the Pd-mediated decarboxylation process of aryl carboxylic acids. *Dalton Trans.* **2010**, 39, 9815–9822.

(33) One of the few studies to examine binding energies of amidate anions versus carboxylate anions is Bordwell's study on alkali metal ion pairing in DMSO, which found that carboxylates bind more strongly than amidates. See: Olmstead, W. N.; Bordwell, F. G. Ion-pair association constants in dimethyl sulfoxide. *J. Org. Chem.* **1980**, *45*, 3299–3305.

(34) This is consistent with the fact that there are many more transition metal carboxylate structures in The Cambridge Structural Database than amidate structures. Groom, C. R.; Bruno, I. J.; Lightfoot, M. P.; Ward, S. C. The Cambridge Structural Database. *Acta Crystallogr., Sect. B: Struct. Sci., Cryst. Eng. Mater.* **2016**, *B72*, 171–179. For a review of coordinated amidates, see ref 18.

(35) Nilsson, P.; Olofsson, K.; Larhed, M. *Microwave Methods in Organic Synthesis*; Springer: Berlin, Heidelberg, 2006.

(36) Savmarker, J.; Rydfjord, J.; Gising, J.; Odell, L. R.; Larhed, M. Direct palladium(II)-catalyzed synthesis of arylamidines from aryltrifluoroborates. *Org. Lett.* **2012**, *14*, 2394–2397.

(37) Rydfjord, J.; Svensson, F.; Trejos, A.; Sjoberg, P. J.; Skold, C.; Savmarker, J.; Odell, L. R.; Larhed, M. Decarboxylative palladium(II)-catalyzed synthesis of aryl amidines from aryl carboxylic acids: development and mechanistic investigation. *Chem. - Eur. J.* **2013**, *19*, 13803–13810.

(38) Sherwood, J.; De Bruyn, M.; Constantinou, A.; Moity, L.; McElroy, C. R.; Farmer, T. J.; Duncan, T.; Raverly, W.; Hunt, A. J.; Clark, J. H. Dihydrolevoglucosenone (Cyrene) as a bio-based alternative for dipolar aprotic solvents. *Chem. Commun.* **2014**, *50*, 9650–9652.

(39) We have also examine the role of TFA for a range of other systems (see Table S2 and Scheme S1 in the Supporting Information) and in all cases the yields are diminished relative to the protocol with no added TFA (Scheme 5).

(40) Drover, M. W.; Schafer, L. L.; Love, J. A. Isocyanate deinsertion from kappa(1)-O amidates: facile access to perfluoroaryl rhodium(I) complexes. *Dalton Trans.* **2015**, *44*, 19487–19493.

(41) The protodecarboxylation pathway may proceed via protonation by 2,6-dimethoxybenzoic acid instead of TFA; however, we have not attempted to model this pathway.

(42) We have been unable to locate transition structures connecting **19f** and **20f**. Subsequent DFT calculations (Figure 8) indicates that protodemetalation likely proceeds through **19f**, with **20f** lying off cycle.

(43) Woolley, M. J.; Khairallah, G. N.; da Silva, G.; Donnelly, P. S.; Yates, B. F.; O'Hair, R. A. J. Role of the Metal, Ligand, and Alkyl/Aryl Group in the Hydrolysis Reactions of Group 10 Organometallic Cations [(L)M(R)]<sup>+</sup>. *Organometallics* **2013**, *32*, 6931–6944.

(44) Woolley, M.; Khairallah, G. N.; da Silva, G.; Donnelly, P. S.; O'Hair, R. A. J. Direct versus Water-Mediated Protodecarboxylation of Acetic Acid Catalyzed by Group 10 Carboxylates, [(phen)M(O<sub>2</sub>CCH<sub>3</sub>)]<sup>+</sup>. *Organometallics* **2014**, *33*, 5185–5197.

(45) Woolley, M.; Ariafard, A.; Khairallah, G. N.; Kwan, K. H.-Y.; Donnelly, P. S.; White, J. M.; Cauty, A. J.; Yates, B. F.; O'Hair, R. A. J. Decarboxylative-Coupling of Allyl Acetate Catalyzed by Group 10 Organometallics, [(phen)M(CH<sub>3</sub>)]<sup>+</sup>. *J. Org. Chem.* **2014**, *79*, 12056–12069.

(46) Donald, W. A.; McKenzie, C. J.; O'Hair, R. A. J. C-H Bond Activation of Methanol and Ethanol by a High-Spin FeIVO Biomimetic Complex. *Angew. Chem., Int. Ed.* **2011**, *50*, 8379–8383.

(47) Lam, A. K. Y.; Li, C.; Khairallah, G.; Kirk, B. B.; Blanksby, S. J.; Trevitt, A. J.; Wille, U.; O'Hair, R. A. J.; da Silva, G. Gas-phase reactions of aryl radicals with 2-butyne: experimental and theoretical investigation employing the N-methyl-pyridinium-4-yl radical cation. *Phys. Chem. Chem. Phys.* **2012**, *14*, 2417–2426.

(48) Sheldrick, G. SHELXT - Integrated space-group and crystal-structure determination. *Acta Crystallogr., Sect. A: Found. Adv.* **2015**, *A71*, 3–8.

(49) Sheldrick, G. Crystal structure refinement with SHELXL. *Acta Crystallogr., Sect. C: Struct. Chem.* **2015**, *C71*, 3–8.

(50) Dolomanov, O. V.; Bourhis, L. J.; Gildea, R. J.; Howard, J. A. K.; Puschmann, H. OLEX2: a complete structure solution, refinement and analysis program. *J. Appl. Crystallogr.* **2009**, *42*, 339–341.

(51) Frisch, M. J.; Trucks, G. W.; Schlegel, H. B.; Scuseria, G. E.; Robb, M. A.; Cheeseman, J. R.; Scalmani, G.; Barone, V.; Mennucci, B.; Petersson, G. A.; Nakatsuji, H.; Caricato, M.; Li, X.; Hratchian, H. P.; Izmaylov, A. F.; Bloino, J.; Zheng, G.; Sonnenberg, J. L.; Hada, M.; Ehara, M.; Toyota, K.; Fukuda, R.; Hasegawa, J.; Ishida, M.; Nakajima, T.; Honda, Y.; Kitao, O.; Nakai, H.; Vreven, T.; Montgomery, J. A., Jr.; Peralta, J. E.; Ogliaro, F.; Bearpark, M.; Heyd, J. J.; Brothers, E.; Kudin, K. N.; Staroverov, V. N.; Kobayashi, R.; Normand, J.; Raghavachari, K.; Rendell, A.; Burant, J. C.; Iyengar, S. S.; Tomasi, J.; Cossi, M.; Rega, N.; Millam, J. M.; Klene, M.; Knox, J. E.; Cross, J. B.; Bakken, V.; Adamo, C.; Jaramillo, J.; Gomperts, R.; Stratmann, R. E.; Yazyev, O.; Austin, A. J.; Cammi, R.; Pomelli, C.; Ochterski, J. W.; Martin, R. L.; Morokuma, K.; Zakrzewski, V. G.; Voth, G. A.; Salvador, P.; Dannenberg, J. J.; Dapprich, S.; Daniels, A. D.; Farkas, Ö.; Foresman, J. B.; Ortiz, J. V.; Cioslowski, J.; Fox, D. J. *Gaussian 09, Revision D.01*; Gaussian, Inc.: Wallingford, CT, 2009.

(52) Zhao, Y.; Truhlar, D. G. The M06 suite of density functionals for main group thermochemistry, thermochemical kinetics, non-covalent interactions, excited states, and transition elements: two new functionals and systematic testing of four M06-class functionals and 12 other functionals. *Theor. Chem. Acc.* **2008**, *120*, 215–241.

(53) Hay, P. J.; Wadt, W. R. Ab initio effective core potentials for molecular calculations. Potentials for the transition metal atoms Sc to Hg. *J. Chem. Phys.* **1985**, *82*, 270–283.

(54) Wadt, W. R.; Hay, P. J. Ab initio effective core potentials for molecular calculations. Potentials for main group elements Na to Bi. *J. Chem. Phys.* **1985**, *82*, 284–298.

(55) Hariharan, P. C.; Pople, J. A. The influence of polarization functions on molecular orbital hydrogenation energies. *Theor. Chim. Acta* **1973**, *28*, 213–222.

(56) Ehlers, A. W.; Böhme, M.; Dapprich, S.; Gobbi, A.; Höllwarth, A.; Jonas, V.; Köhler, K. F.; Stegmann, R.; Veldkamp, A.; Frenking, G. A set of *f*-polarization functions for pseudo-potential basis sets of the transition metals ScCu, YAg and LaAu. *Chem. Phys. Lett.* **1993**, *208*, 111–114.

(57) Höllwarth, A.; Böhme, M.; Dapprich, S.; Ehlers, A. W.; Gobbi, A.; Jonas, V.; Köhler, K. F.; Stegmann, R.; Veldkamp, A.; Frenking, G. A set of *d*-polarization functions for pseudo-potential basis sets of the main group elements AlBi and *f*-type polarization functions for Zn, Cd, Hg. *Chem. Phys. Lett.* **1993**, *208*, 237–240.

(58) Barone, V.; Cossi, M. Quantum Calculation of Molecular Energies and Energy Gradients in Solution by a Conductor Solvent Model. *J. Phys. Chem. A* **1998**, *102*, 1995–2001.

(59) Becke, A. D. Density-functional exchange-energy approximation with correct asymptotic behavior. *Phys. Rev. A: At., Mol., Opt. Phys.* **1988**, *38*, 3098–3100.

(60) Lee, C.; Yang, W.; Parr, R. G. Development of the Colle-Salvetti correlation-energy formula into a functional of the electron density. *Phys. Rev. B: Condens. Matter Mater. Phys.* **1988**, *37*, 785–789.

(61) Becke, A. D. Density-functional thermochemistry. III. The role of exact exchange. *J. Chem. Phys.* **1993**, *98*, 5648–5652.

(62) Stephens, P. J.; Devlin, F. J.; Chabalowski, C. F.; Frisch, M. J. Ab Initio Calculation of Vibrational Absorption and Circular Dichroism Spectra Using Density Functional Force Fields. *J. Phys. Chem.* **1994**, *98*, 11623–11627.

(63) Weigend, F.; Furche, F.; Ahlrichs, R. Gaussian basis sets of quadruple zeta valence quality for atoms H-Kr. *J. Chem. Phys.* **2003**, *119*, 12753–12762.

(64) Okuno, Y. Theoretical Investigation of the Mechanism of the Baeyer-Villiger Reaction in Nonpolar Solvents. *Chem. - Eur. J.* **1997**, *3*, 212–218.

(65) Keith, J. A.; Carter, E. A. Quantum Chemical Benchmarking, Validation, and Prediction of Acidity Constants for Substituted Pyridinium Ions and Pyridinyl Radicals. *J. Chem. Theory Comput.* **2012**, *8*, 3187–3206.